Geoderma 338 (2019) 14–29

Contents lists available at ScienceDirect

Geoderma

journal homepage: www.elsevier.com/locate/geoderma

Controls of the spatial variability of denitrification potential in nontidal floodplains of the Chesapeake Bay watershed, USA

Alicia R. Korol[a,*], Gregory B. Noe[b], Changwoo Ahn[a]

[a] Department of Environmental Science and Policy, George Mason University, 4400 University Drive, Fairfax, VA 22030, USA
[b] Hydrological-Ecological Interactions Branch, United States Geological Survey, 430 National Center, Reston, VA 20192, USA

ARTICLE INFO

Handling Editor: Jan Willem Van Groenigen

Keywords:
Biogeochemistry
Floodplain sedimentation
Floodplain soils
Hydrogeomorphology
Land cover
Nitrogen

ABSTRACT

Identifying floodplains with high rates of denitrification will help prioritize restoration projects for the removal of nitrogen. Currently, relationships of denitrification with hydrogeomorphic, physiographic, and climate (*i.e.*, largescale) characteristics of floodplains are relatively unknown, even though these characteristics have datasets (*e.g.*, geographic mapping tools) that are publicly available (or soon-to-become) that could be used to understand denitrification variability. Thus, we investigated control of denitrification by these largescale characteristics in eighteen nontidal floodplains of the Chesapeake Bay watershed (*i.e.*, at regional scale, > 100 km, scale), using measurements or compiled data at the scales of the stream reach and respective catchment; floodplain soil and herbaceous vegetation (*i.e.*, local) characteristics were additionally investigated. Soil denitrification potentials were measured in May, July, and August using complementary acetylene-based techniques under an anoxic environment. Linear largescale predictors of denitrification potential measurements included stream nitrogen and phosphorus concentrations (+), channel width-to-depth ratio (+), floodplain sedimentation (+), forested (−) and urban (+) catchment land cover, and seasonal air temperature (−). Three predictors, catchment forested land cover (strongly related to agricultural land cover), catchment urban land cover, and floodplain sedimentation were related to the most number of denitrification potential measurements. Soil structure, soil nutrient concentrations, and herbaceous vegetation characteristics that were seasonally measured (with a few exceptions) were linear predictors of denitrification potentials in May and August, with nitrogen and carbon characteristics the most consistent (positive) predictors across measurements. Nutrient amendment assays further supported the importance of nitrogen and carbon controls. Using the local characteristics as statistical mediators in path analysis, greater non-forested catchment land cover indirectly increased denitrification through greater floodplain soil nitrate, total phosphorus, and herbaceous aboveground biomass. Additionally, greater floodplain sedimentation indirectly increased denitrification through greater soil pH, total phosphorus, and potential carbon mineralization. Due to the consistency of relationships across denitrification potential measurements along with path modeling results, hotspots of floodplain denitrification should be found in urban and agricultural catchments where river-floodplain hydrologic connectivity promotes sedimentation. Largescale predictors explained 43–57% of the variation in denitrification potentials and should be useful for prediction in floodplains. Siting restoration projects in watersheds for maximum nitrate removal using publicly available largescale datasets is both feasible and effective.

1. Introduction

Denitrification removes large portions of diffuse anthropogenic nitrogen (N) from the biosphere and mitigates the negative impacts of excess N on ecosystem functioning in local and downstream environments (Fowler et al., 2013). Soils and sediments with high rates of denitrification promote the microbially-mediated anerobic process with adequate N and carbon (C) supply and favorable physicochemical conditions (*i.e.*, pH and temperature) (Robertson and Groffman, 2015). Because the anoxic soils of floodplains can intercept large amounts of excess N transported by groundwater and surface water, the primary substrate for denitrification, restoration of degraded floodplains has been promoted to augment nutrient reductions (*e.g.*, denitrification) at the scale of watersheds (U.S. EPA, 2010). Floodplain management to increase nutrient removal has included reverting floodplains to unmanaged (*e.g.*, non-cropped) land use, improving frequency and

* Corresponding author.
E-mail address: alikor23@gmail.com (A.R. Korol).

https://doi.org/10.1016/j.geoderma.2018.11.015
Received 2 April 2018; Received in revised form 11 October 2018; Accepted 7 November 2018

stability of hydrologic connectivity, and prioritizing restoration sites in a landscape to maximize benefits to the surrounding watershed (*e.g.*, a watershed approach) (Zedler, 2003; Opperman et al., 2010; Chabot et al., 2016). Current uncertainty in identifying floodplains with high rates of denitrification due to environmental heterogeneity limits the targeting of sites for conservation or restoration and creates the need for further study on the predictors of denitrification conducted at large spatial scales (Heffernan et al., 2014; van Groenigen et al., 2015).

A call for more research on floodplain denitrification has been made for the Chesapeake Bay watershed, which drains > 165,000 km^2 across the mid-Atlantic United States; the research studies on predictors and controls of denitrification that have been conducted have been localized (*i.e.*, the area between the cities of Washington D.C. and Baltimore M.D.) and thus have not incorporated the largescale landscape heterogeneity that may be of importance to denitrification rates at larger scales (Berg et al., 2014). For instance, soil characteristics and groundwater flow vary greatly across the watershed's five major physiographic provinces from the local influences of land use, topography, climate, parent material and a patchwork of differing lithologies (Bachman et al., 1998; Sherwood and Garst, 2016). In addition, continental position acting together with physiographic region (*e.g.*, altitude) give rise to numerous ecoregions in the watershed within the broader humid temperate climate (Bailey, 2009). Recent studies conducted at small scales in specific land use classes or physiographic areas (< 100 km; *e.g.*, Tomasek, 2017) nonetheless provide good evidence for certain controls of denitrification but need to be tested for importance at the scale of the watershed. Ultimately, improved understanding and prediction of the impact of floodplains on downstream N loading will benefit implementation of the regulatory total maximum daily load of N for the Chesapeake Bay watershed (76 Fed. Reg. 549).

High variability in the direct regulation of denitrification primarily contributes to the uncertainty of rates in floodplains (Vidon et al., 2010). Oxygen becomes highly limited in the saturated surface soils of floodplains, and thus saturation, as a proxy of oxygen availability, largely predicts denitrification activity (McClain et al., 2003; Burgin et al., 2010; Messer et al., 2012). Though low N availability often limits ecosystem functioning (*e.g.*, denitrification), N becomes more available from anthropogenic influence (*e.g.*, urban developments or agriculture) in a watershed (Forshay and Stanley, 2005; Schilling and Lockaby, 2005; Antheunisse et al., 2006), which in turn begets greater C demand by denitrifiers (Groffman and Crawford, 2003; Rivett et al., 2008; Welsh et al., 2017). Temperature and pH further directly regulate denitrification through physicochemical constraints on biochemical reactions and the availability of N and C in the soil (Mitsch and Gosselink, 2015). Because the metabolic functioning (*e.g.*, gene expression) of denitrifiers requires a circumneutral pH, reports of relatively low pH values (*e.g.*, < 5) in floodplains (Ashby et al., 1998; Saleh-Lakaha et al., 2009) should exert strong control on the spatial variability of the process.

Particularly at large scales, certain environmental characteristics (*e.g.*, hydrologic connection, land use, climate) may be able to integrate the multiple effects, non-linearities, and long-term interactions of denitrification with its direct biogeochemical controls for more effective and efficient prediction of denitrification (*e.g.*, Harms and Grimm, 2008). Environmental characteristics that indirectly affect denitrification in floodplains can be conceptualized in a nested, hierarchical, spatial framework, whereby hydrogeomorphic processes – water flow, groundwater storage, and sediment and nutrient movement – predominantly regulate ecosystem interactions (Fig. 1; Thoms and Parsons, 2002, Noe, 2013). Denitrification in floodplains increases with finer soil textures that retain moisture (reducing oxygen levels) and can coincide with areas of greater organic matter and pH, which in turn are associated with morphological features of the floodplains (*e.g.*, depressions) (Pinay et al., 2000; Welsh et al., 2017; Pahlavan-Rad and Akbarimoghaddam, 2018). The type and productivity of the vegetation community, also responsive to floodplain hydrologic regime (Wassen et al., 2002), influence denitrification by adjusting soil nutrient pools (*e.g.*, increasing C), reducing temperature, and increasing redox (Sutton-Grier et al., 2013; Korol et al., 2016). Notably, hydrogeomorphic processes can regulate the effect of vegetation on denitrification where long-term flooding stymies the accumulation of soil organic C by the erosion of organic litter and burial/disturbance of plant shoots by mineral sediment (Cabezas and Comín, 2010; Saint-Laurent et al., 2016). Specific to biogeochemical cycling, hydrologic connectivity between river and floodplains, involving material exchange from groundwater or surface water, directly promotes nutrient cycling and creates a large potential for anaerobic processes in floodplains relative to upland areas (Hill et al., 2000; Hefting et al., 2004; Duncan et al., 2013). Short pulses of high denitrification rates occur after flooding due to reduced redox potential, elevated dissolved organic C, and nitrate inputs (Forshay and Stanley, 2005; Shrestha et al., 2014). Long-term pulses occur in zones with higher groundwater levels, longer residence times, and sediment inputs (Hefting et al., 2004; McPhillips et al., 2015; McMillan and Noe, 2017).

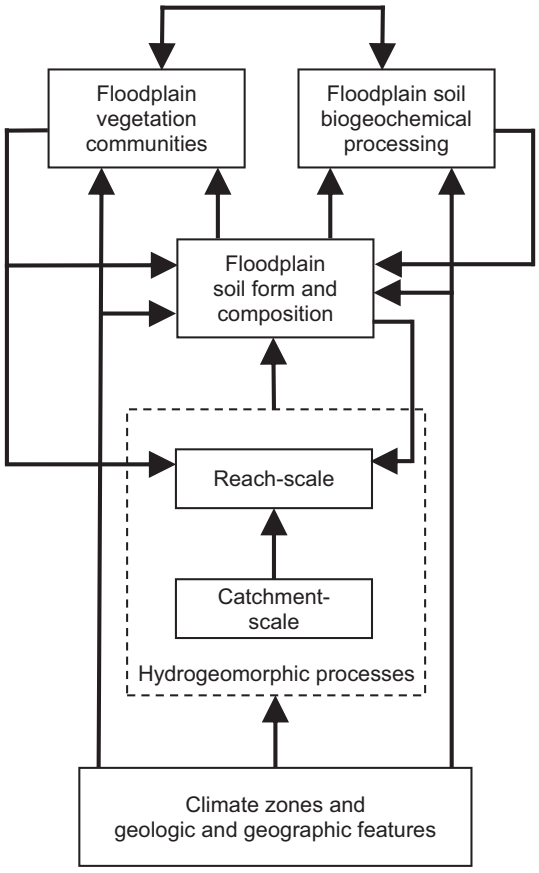

Fig. 1. Conceptual model of the expected controls of denitrification and other biogeochemical processes in floodplains. Floodplain ecosystems are comprised of the physical habitat, vegetation community, and biogeochemical processes, all which interact spatially within the limits of the floodplain. Reach-scale hydrogeomorphic processes, mediated by the morphometry and composition of the physical habitat and the structure and activity of the vegetation community, create interactions between floodplain components and the stream and upland areas; biogeochemical mediation of reach-scale processes are considered negligible for this study. Catchment-scale hydrogeomorphic processes drive nested reach-scale processes through upstream-downstream and upland-stream connections. Floodplain components and hydrogeomorphic processes are all influenced by climate zones and geologic and geographic features.

At reach or segment scales of a river network, floods and sediment supply to the floodplain are influenced by the underlying geomorphic template of the stream valley (*e.g.*, stream slope, channel geometry, fine sediment storage, and bedrock constraint) (Rosgen, 1994; Gordon et al.,

2004). Less incised streams, or wide or shallow geometry, spill onto the floodplains more frequently, promoting hot moments of denitrification (Bernard-Jannin et al., 2017), while floodplain zones of highest sedimentation and potential for nutrient deposition include stream banks, swales, and abandoned channels (Kaase and Kupfer, 2016). These local hydrogeomorphic processes are in turn spatially nested within hydrogeomorphic processes of the larger river basin (Lowrance et al., 1997; Winter, 2001; McCluney et al., 2014).

Upland human land use degrades hydrogeomorphic processes of river basins and modifies natural floodplain N cycling (Groffman et al., 2002; Allan, 2004). Concentrated upstream areas of urban or agricultural development alter natural flooding regimes and increase nutrient and sediment inputs to floodplains (Noe and Hupp, 2005; Gellis et al., 2009). Urban streams are often characterized by more powerful and flashier discharges after storm events, which can increase the frequency of high energy, short duration floodplain inundation (Hupp et al., 2013; Hopkins et al., 2015). Highly energetic storm flow further lowers base flow and riparian groundwater tables and can increase channel-floodplain disconnection through greater channel incision (Walsh et al., 2005; Schwartz et al., 2012). Though less hydrologic connection impedes denitrification, floodplains in urban and agricultural catchments can still exhibit equal or higher rates of denitrification potential as floodplains in forested catchments (Groffman and Crawford, 2003; Harrison et al., 2011; Waters et al., 2014), and thus spatial variability of floodplain denitrification potential in floodplains should positively relate to non-forested land cover across catchments.

We established four study objectives to identify controls of spatial variability in denitrification potential of surface soils of nontidal floodplains at large spatial scale (*e.g.*, the Chesapeake Bay watershed): (1) investigate bivariate relationships of denitrification potential (measured using complementary laboratory methods) with environmental characteristics (either measured or publicly available); (2) identify more robust predictors of denitrification from those previously identified by considering hierarchical spatial frameworks (Thorp et al., 2006; Fig. 1) and multi-variable relationships; (3) determine whether the previously identified largescale predictors directly or indirectly influence denitrification potential through their influence on local characteristics (Fig. 2); and (4) evaluate the explanatory power of the collective largescale predictors and compare that with the explanatory power of the collective local predictors to inform statistical models of denitrification potential applied at regional scale (> 100 km). While controlling for spatial dependence, we tested for predictors of denitrification potential using soil biogeochemical characteristics, floodplain vegetation, hydrogeomorphic characteristics of the floodplain-channel ecosystem, and catchment land cover, climate, and physiographic location. Because N and C are strong direct controls on the process, we additionally tested for their limiting effects on its spatial variability. For our second objective, we focused our analysis on "largescale" predictors – defined as the hydrogeomorphic characteristics of river reaches (including stream water quality), and the morphometric, land use, and physical characteristics of catchments (*i.e.*, the sub-basins of the Chesapeake Bay watershed) – because the growing availability in geospatial datasets of largescale characteristics (Carbonneau et al., 2012) enables extrapolation of floodplain denitrification over broad spatial extents useful to N modeling and management. Our third and fourth objectives were to provide greater theoretical and practical support to findings from our first two objectives. Regarding the third objective, we tested for statistical mediation using the floodplain soil and vegetation characteristics as they are also strongly controlled by hydrogeomorphic, physiographic, and climatic processes (Thorp et al., 2006, Noe, 2013; Fig. 1). We used path models that account for these multiple causal effects, as well as the reciprocal effects that vegetation, and the form and composition of soil (*e.g.*, texture) have on hydrogeomorphic processes by moderating sediment flux and soil moisture (Noe, 2013; Harvey and Gooseff, 2015). Finally, we examined our outcomes in two seasons to determine the consistency of spatial controls on denitrification potential across variable discharge scenarios.

We expected that the patterns in denitrification potential would follow largescale characteristics that exert strong influence over direct, process-related controls of denitrification: characteristics related to more hydrologic connectivity, N delivery, soil C accumulation, or higher pH in floodplains.

2. Methods

2.1. Floodplain sites and plots

Eighteen forested floodplains associated with the USGS Chesapeake Floodplain Network and adjacent USGS Nontidal Network of river gage and load stations in the Chesapeake Bay watershed were selected for study (Fig. 2). Floodplains span the lower central region of the watershed (37°58′–40°21′N; 75°56′–78°39′W), all within 180 km of George Mason University (Fairfax, VA). Sites were selected to capture broad-scale heterogeneity in drainage area, land use, geology and topography (Fig. 2, Table 1). For physiographic heterogeneity, the 18 sites were evenly distributed across the Coastal Plain, Piedmont, and Valley and Ridge physiographic provinces (*i.e.*, 6 sites/province). Sites were then further distributed in the provinces across gradients of soil physicochemical properties, land cover classes, and hydrogeomorphic heterogeneity, and roughly in that order of influence. Data on soil physicochemical properties were available for 30 USGS Chesapeake Floodplain Network sites in the Ridge and Valley and Piedmont provinces at the time of our study design, which we clustered into subgroups to help select this study's sites across a range of soil conditions. Two sites each were then selected to have high relative percentages of either of three land cover classes, *i.e.*, urban, agricultural, or forested. Finally, for hydrogeomorphic heterogeneity, sites were associated with a range in catchment size (10^1–10^3 km^2). Sampling in two seasons – spring and summer – for the majority of denitrification, soil, and vegetation characteristics also captured heterogeneity in relative stream-floodplain connectivity because evaporation and plant transpiration can lower stream flow to an annual minimum by late summer (Cummins et al., 2010).

At each site, a floodplain transect was established on one bank running perpendicular from the stream to the base of the toe slope. Four sampling point locations (= plots) were established at unique geomorphic features of the floodplain, including the natural levee and the base of the toe-slope, and additional locations such as depressions or areas of abrupt change in vegetation or elevation. Due to the narrowness and homogeneity of the floodplain cross-section for two sites (*i.e.*, Antietam Creek, MD, and Warm Spring Run, WV), one of the plots was placed on the opposite bank, behind the natural levee, ensuring greater variation in sampling. All denitrification potentials and most soil and vegetation characteristics of the floodplain were measured at these four plots/site. For the specific denitrification measurements made in August (and not May or July) 2016, we expanded our sampling to a fifth plot located along the transect at 9 randomly selected sites to more thoroughly capture within-site variability of denitrification (*i.e.*, to increase sample size per site).

A second transect was established roughly 100 m apart from the first transect. This second transect, along with the primary transect for this study, was used in the measurements of a few soil and site morphometric characteristics (described below) that took place between 2013 and 2015. For the specific measurements occurring among these two transects, floodplains on both sides of the stream were sampled where present.

2.2. Field collections of soil and vegetation

The bulk of measurements on denitrification potential and soil and vegetation characteristics of the floodplain occurred in May and August

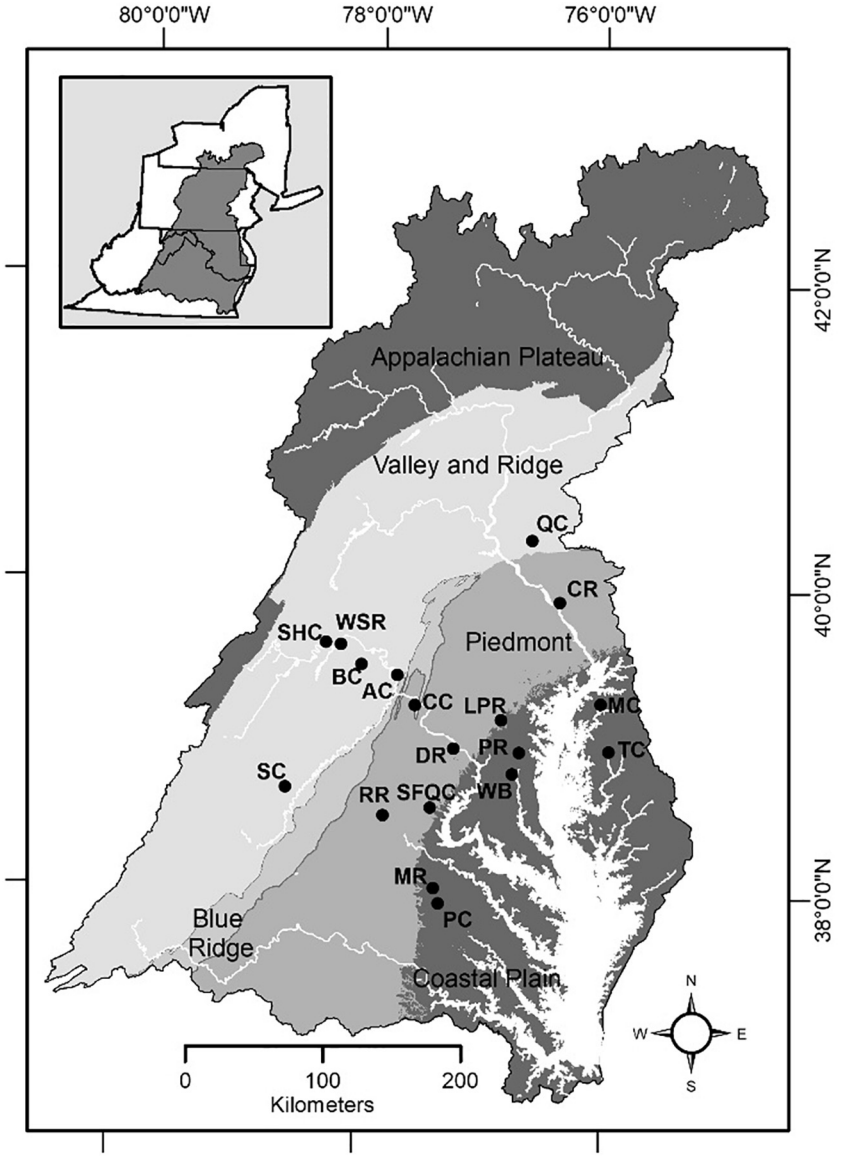

Fig. 2. Eighteen nontidal floodplain sites within three physiographic provinces of the Chesapeake Bay watershed. Site acronyms: Antietam Creek (AC), Back Creek (BC), Catoctin Creek (CC), Conestoga River (CR), Difficult Run (DR), Little Patuxent River (LPR), Mattaponi River (MR), Morgan Creek (MC), Patuxent River (PR), Polecat Creek (PC), Quittapahilla Creek (QC), Rappahannock River (RR), Sideling Hill Creek (SHC), Smith Creek (SC), South Fork Quantico Creek (SFQC), Tuckahoe Creek (TC), Warm Springs Run (WSR), Western Branch (WB).

of 2016. In both months, we collected soils to measure two different denitrification potentials along with physicochemical properties (*i.e.*, bulk density, moisture, pH, N, C, organic matter, and extractable nitrate, ammonium, orthophosphate and their ratios) and processes (*i.e.*, potential C mineralization flux). In July, we also collected soils for a substrate limitation experiment of denitrification potential (using a third, but related method) and took measurements of above- and belowground vegetation. In each sampling month, soils were retrieved during a contiguous 7- to 9-day period and refrigerated each evening. We sampled for vegetation and soils perpendicular to the floodplain transect within 5 m of the denitrification plot. Soil cores (2.1 cm diameter), with the exception of root biomass cores, were collected to 10 cm because more concentrated organic matter in the upper horizons of the soil was expected to stimulate the highest rates of denitrification potential with greater available N and C (Welsh et al., 2017).

2.3. Denitrification potential measurements

We measured denitrification in the week immediately following soil collection. Denitrification potentials were measured with laboratory incubations using more than one technique but always in a 10% acetylene/N_2 headspace to inhibit N_2O reduction to N_2 (Knowles, 1990). In all, we made seven measurements of denitrification from every plot. All gas samples were held in 10 mL glass vials with aluminum caps and butyl rubber septa for a maximum of 2 days prior to analysis for N_2O using electron capture gas chromatography and a Hayesep Q 80/100 packed column (Shimadzu GC-8A).

In May and August, we measured denitrification enzyme activity (DP_{DEA}) from nitrate- and C-amended, saturated soil slurries. Our procedure followed Groffman et al. (1999). Soil-solution mixtures were formed with 25 g field moist soil (from triplicate soil cores) in 25 mL media comprised of potassium nitrate (1.01 g/L), dextrose (1.80 g/L), chloramphenicol (0.1 g/L), and deionized water. Slurries were bubbled with N_2 prior to incubations to remove oxygen. Gas samples were withdrawn at 45 and 105 min after the injection of acetylene. We expressed DP_{DEA} rates as $\mu g\text{-}N\,kg^{-1}\,h^{-1}$ on the basis of dry soil after adjusting for soil moisture.

We also measured denitrification potential in static, whole cores

Table 1
Characteristics of 18 floodplain sites selected for study associated with U.S. Geological Survey stream gage and load stations.

USGS gage #	Site acronyms[1]	Catchment % forested land cover[2]	Catchment % urban land cover[2]	Catchment % agricultural land cover[2]	Floodplain sedimentation ($g\,m^{-2}\,yr^{-1}$)	Floodplain soil mois-ture ($g\,g^{-1}$)[3]	Floodplain % soil N[3]	Floodplain soil pH[3]	Floodplain AGB ($g\,m^{-2}$)[4]
01619500	AC	32	13	54	3384	0.39	0.26	7.64	88
01614000	BC	77	4	18	3871	0.27	0.13	6.04	136
01638480	CC	33	6	60	247	0.29	0.12	6.07	213
01576754	CR	24	25	48	2782	0.36	0.19	7.17	103
01646000	DR	37	57	2	4159	0.29	0.09	5.62	70
01593500	LPR	20	66	10	2224	0.31	0.18	5.18	165
01674000	MR	70	4	14	453	0.40	0.18	4.80	43
01493500	MC	2	1	91	1306	0.41	0.14	5.12	143
01594440	PR	33	32	27	1289	0.45	0.23	5.80	50
01674182	PC	68	8	14	564	0.50	0.15	5.17	104
01573160	QC	16	31	51	2915	0.43	0.32	7.60	485
01664000	RR	61	3	35	2176	0.37	0.18	5.82	181
01610155	SHC	81	2	17	1315	0.22	0.10	4.84	75
01632900	SC	47	8	45	12,127	0.39	0.32	7.63	83
01658500	SFQC	87	2	1	1424	0.31	0.11	4.70	39
01491500	TC	15	1	68	882	0.08	0.06	5.99	74
01613030	WSR	60	28	11	0	0.34	0.19	6.56	123
01594526	WB	31	51	11	14,948	0.64	0.16	6.04	138

Notes:
[1]See Fig. 2 for descriptions and locations.
[2]Chesapeake Conservancy (2017).
[3]Mean seasonal measurements in this study.
[4]Abbreviations: AGB = herbaceous aboveground biomass.

either at field moisture (for May and August samplings) or at saturation (July sampling for a substrate limitation experiment) (Groffman et al., 1999). Extracted whole soil cores were placed in acrylic tubes (20.3 × 2.2 cm inner diameter) in the field and held capped and refrigerated in the lab until analysis. Caps on the tubes were replaced with rubber stoppers prior to flushing the headspace with N_2. For denitrification potential from field moist soil (DP_{FM}), cores were incubated in the dark after acetylene addition and sampled at 4 and 8 h. Unlike DP_{DEA}, DP_{FM} reflects the strong influence of short-term soil structure and composition on denitrification, and relatedly, the spatial discontinuity and limitations in moisture, nitrate, and organic C. DP_{DEA}, by contrast, measures enzyme activity of denitrifiers with no direct substrate limitation and correlates well with long-term rates of denitrification (Groffman et al., 1992). Finally, a substrate limitation test was conducted with saturated static cores and three treatments: saturation (DP_S), saturation with nitrate (DP_{SN}), and saturation with nitrate and C (DP_{SNC}). Media solutions were prepared with the same potassium nitrate and dextrose concentrations used for DP_{DEA} measurement. Cores were submerged in 15 mL of solution (for no longer than 20 min) prior to the start of the incubation with headspace adjustment and sampled at 4 and 8 h afterwards. Denitrification potential in field moist cores and saturated measurements were expressed by soil volume as $\mu g\,N\,m^{-3}\,h^{-1}$.

2.4. Floodplain soil and vegetation measurements

Soil gravimetric moisture, measured from one dedicated soil core, and bulk density, measured using a slide hammer and plastic sleeves (9.9 × 4.7 cm), were measured immediately within the week of sampling. Soils were dried at 105 °C for 48 h for moisture (Gardner, 1996), expressed as $g\,g^{-1}$, and over 72 h for bulk density, expressed as $g\,cm^{-3}$ (Blake and Hartge, 1986).

Triplicate soil cores per plot were specifically collected for organic matter, total C, total N, and pH, and were air dried after the soil collection period. Soils were then ground and sieved to < 2 mm. For organic matter, measured by mass loss on ignition, ~2 g soil subsample was dried to 105 °C for 24 h prior to ignition in a muffle furnace (Thermo Fisher Scientific, Thermolyne) at 550 °C for 4 h ($g\,g^{-1}$; Nelson and Sommers, 1996). For C and N, a separate subsample of soil was dried at 105 °C for 24 h immediately prior to analysis of 12–18 mg of soil using dry combustion in an elemental analyzer (% of dry soil; Perkin Elmer 2400 Series II; Nelson and Sommers, 1996). Soil pH was measured in a 1:2 ratio of soil to deionized water (Robertson et al., 1999a), with the soil slurries shaken vigorously and allowed to settle for 30 min prior to taking measurement of the solution with a hand-held sensor (Thermo Fisher Scientific, Fisherbrand accumet AP 110).

Two soil cores per plot were retrieved for potential C mineralization in the spring only and were refrigerated until analysis. We used short-term measurements with field moist soils as an index of "immediately-available" C (Robertson et al., 1999b). We placed 20 g of dry-weight equivalent field moist soil (mean water-filled pore space of soils = 74%) into 360 cm^3 glass jars and let the soils equilibrate to room temperature overnight. We measured CO_2 flux ($mmol\text{-}CO_2\ kg\text{-}dw^{-1}\,h^{-1}$) over 2 min, twice per plot, using a LI-COR 8100A automated soil gas flux system adapted for use with small chambers (Craft et al., 2003).

For measurements of soil ammonium, nitrate, and orthophosphate (SRP: soluble reactive P), salt extractions (Robertson et al., 1999b) on dedicated duplicate soil cores per plot occurred no later than 3 days following collection from each floodplain site. Six grams of field moist soil was mixed with 40 mL of 2 M KCL on a shaker table for an hour then allowed to gravity separate for 30 min. Supernatant was filtered through an Acrodisc syringe filter with a Supor 0.45 μm membrane and measured photometrically on a discrete analyzer (SEAL analytical, AQ2) along with 2 M KCl blanks and an external standard (ERA, Arvada, Colorado, USA). Measured concentrations of N or P were expressed as $\mu g\text{-}N\ g\text{-}dw^{-1}$ or $\mu g\text{-}P\ g\text{-}dw^{-1}$.

We measured three characteristics of the plant community: herbaceous cover, herbaceous aboveground biomass (AGB), and belowground biomass (BGB). Total percent cover of the herbaceous plant community (and woody plants < 1 m tall) was measured in 1 × 2 m grids using 11 cover classes (Tiner, 1999). Cover class midpoints per plot were used for further statistical analysis. Aboveground herbaceous biomass was harvested within a 1 m^2 grid and placed in paper bags. Soil cores (6.4 cm diameter; 30 cm depth) for analysis of belowground biomass (Bledsoe et al., 1999) were held in plastic bags and refrigerated until roots ≥ 2 mm were washed and sieved from the soil. Plant biomass was dried at 60 °C to constant mass for measurement of dry weight (g-

dw m^{-2}).

Three other soil characteristics were measured either *in situ* or prior to 2016 in the laboratory. To measure soil temperature, iButton thermistors (Embedded Data Systems) were deployed at the end of May to three plots (levee, adjacent to levee, and base of toe-slope) at a depth of 5–10 cm, recording at 90 min intervals, and retrieved during the August collection (beginning of month). Mean maximum daily soil temperatures were calculated for June and July. Soil total P (mg per g dry soil; microwave assisted strong acid digestion followed by ICP-OES analysis; Falciani et al., 2000, CEM Discovery SP-D), bulk density (used in the calculation of total P), and the proportion of soil particles smaller than 63 μm were measured by laser diffraction analysis (Beckman Coulter LS 13320) once in previous years (2013–2015) at six locations (5 cm depth) spread among the primary and secondary transects at each site. The seasonal soil C and N combined with the P measurements were used to calculate soil nutrient mass ratios: C:N, C:P, and N:P.

2.5. Measurements and datasets for hydrogeomorphic, catchment-scale, and physical characteristics

We used datasets on the following hydrogeomorphic characteristics that were compiled or measured within the three years preceding the soil sampling that occurred in 2016: stream discharge and nutrient concentrations (used as estimates of nutrient concentrations in groundwater or nutrient inputs to floodplains from floodwater), floodplain sedimentation, channel and floodplain morphometry metrics, and stream slope. Mean three-year discharge (m^3/s) for water years 2014, 2015, and 2016 from the gage in the measurement reach was retrieved from the USGS National Water Information System (USGS, 2016). Mean stream concentrations (mg/L) of total N and P, measured up to three times per month, were retrieved for the same three-year period from the Chesapeake Bay Program Water Quality Database (CB Program, 2012). Water quality data were screened for duplicate measurements and non-detectable values. Between 2013 and 2015, channel and floodplain morphometric characteristics were measured once at the primary and secondary transects; means were calculated for total floodplain width (bank to toe-slope, both sides), channel width (measured at top of bank), bank height, channel width-to-depth ratio (calculated ratio of channel width and bank height), and entrenchment ratio (calculated ratio of floodplain to channel widths). Long-term net vertical deposition (cm yr^{-1}) on the floodplain was also measured once between 2013 and 2015 using the dendrogeomorphology method (Hupp et al., 2016; mean period of measurement, on the basis of tree age = 45 years; mean number of trees sampled per site = 11) and calculated as a sedimentation rate (g m^{-2} yr^{-1}) using site-specific soil bulk density (0–5 cm). Though these floodplain sedimentation measurements were made prior to the sampling in this study, the dendrogeomorphic rates integrate long-term processes and are likely to be directly comparable to the measured denitrification potential rates (Groffman et al., 1992). River surface water slope (%) was measured using the Stream Channel and Floodplain Metric Toolbox to process 3-m LiDAR-derived DEMs of digital stream reaches (1.5 km in length, on average) (Hopkins et al., 2018).

Catchment-scale and physical characteristics were chosen to reflect regional geographic and land use variability that could affect hydrogeomorphic processes in this study. The datasets for catchment-scale characteristics included the total upstream catchment land cover and morphometry, and sample-site physiographic province, stream elevation, and climate. For this study, we defined the following land cover types using a 1 m^2 resolution dataset: (1) forested = "tree canopy", (2) agriculture = "low vegetation" + "barren", and (3) and urban = "impervious roads" + "impervious surfaces" + "tree canopy over impervious surfaces" (Chesapeake Conservancy, 2017). Catchment area and stream elevation were retrieved from the USGS National Water Information System (USGS, 2016). Physiographic provinces were identified from Bachman et al. (1998). We summarized daily maximum air temperature and total daily precipitation modeled for each floodplain site (PRISM Climate Group, 2017) at two timescales: seasonally (spring: March–May; summer: June–July) and for the year through final sampling (September 2015–August 2016).

2.6. Data analysis

We evaluated all linear relationships between denitrification measurements and the possible explanatory variables (first study objective) using generalized least squares linear models with restricted maximum likelihood to test model fit (Zuur et al., 2009). Mean values were calculated for plots at the site level ($N = 18$), as well as by sampling month, where available (*i.e.*, denitrification potentials, most soil characteristics, and air temperature and precipitation). Largescale characteristics were assessed as predictors of all seven measurements of denitrification potential, while the local characteristics were assessed as seasonal predictors of the denitrification potential measurements of the same period of sampling, with the exception that soil total P and percent silt and clay (measurements from previous years) were assessed as predictors of both May and August DP_{DEA} and DP_{FM} measurements. Logarithmic (base 10) transformations were used on variables to reduce outliers, the spread of data over multiple orders of magnitude, or skew. Transformations were applied consistently across sampling dates on the following: DP_{DEA}, AGB, BGB, soil nitrate, ammonium, and SRP, stream concentrations of N and P, stream discharge, and floodplain sedimentation. We explicitly modeled spatial correlation structures where necessary to account for spatial dependency in the residuals of the linear regression model. The largest model improvement in Akaike's Information Criterion with the inclusion of a structure (*i.e.*, Gaussian, rational, and spherical) was tested for significance (*i.e.*, a violation of spatial independence) with a likelihood ratio test. For the two categorical variables, physiographic province (as a largescale catchment characteristic) and sampling date (for the analysis of temporal variability), we evaluated mean differences in denitrification rates with either the one-way analysis of variance or paired *t*-test, respectively.

Specifically, for our second objective, to identify robust hydrogeomorphic, catchment-scale, and physical predictors, we sought to determine whether relationships of two or more largescale variables with a denitrification potential measurement were related to one underlying cause. Thus, we evaluated associations between statistically significant largescale predictors of the denitrification measurements using Pearson correlation coefficients. In instances of spatially dependent variables, we modeled and interpreted partial regression coefficients on the denitrification measurements.

For our third objective, we applied path analysis to our statistically significant predictors identified from the first two objectives. We evaluated the partial linear effects of the largescale predictors on the denitrification measurements as well as the possible explanations for those partial effects using the local predictors. Models were constructed for denitrification potentials measured in May and August because concurrent soil and vegetation measurements were also available for those months, which was not the case for the July denitrification measurements. The general structure of models (Fig. 3) followed our conceptual model (Fig. 1): models included causal pathways (partial regression coefficients) from largescale predictors to a denitrification measurement, and to a floodplain soil and vegetation predictor to determine the unique effects (effect controlling for other variables' effects: a partial effect) on each of the two response variables. For any vegetation or soil predictor and its mediating effect on hydrogeomorphic variables, we used a reciprocal pathway (partial correlation) that controlled for all other effects in the model instead of a causal pathway (Fig. 3). A reciprocal pathway was also used between the denitrification measurement and soil and vegetation predictor to capture the correlation after controlling for the effects of the largescale variables (Fig. 3). Correlations among the largescale variables are identical to bivariate linear correlations (Fig. 3). For each denitrification measurement and

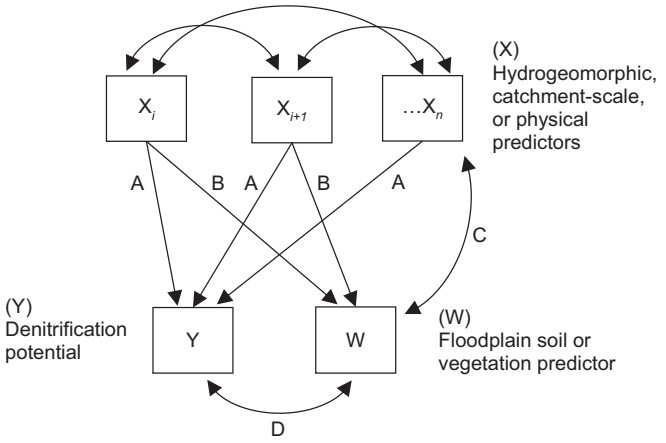

Fig. 3. Statistical model to test for the partial causal effects of multiple largescale (*e.g.*, hydrogeomorphic) predictors on a denitrification potential though paths (A), and on a local (*e.g.*, floodplain soil) predictor of Y causally through paths (B) or causally on but with a reciprocal effect through path (C), and the resulting partial correlation path (D) between Y and W after controlling for the effects of the largescale predictors.

its one or more largescale predictors, we constructed multiple models for each local predictor separately.

To assess the relative explanatory power of the one or more largescale predictors on each denitrification measurement, our fourth objective, we evaluated the total and unique variation explained by the hydrogeomorphic, catchment-scale, and physical predictors compared to the floodplain soil and vegetation predictors using partial redundancy analysis. For use on a single response variable, partial redundancy analysis is a variant of multiple regression that clearly communicates the unique and shared explanatory contribution of two or more groups of predictors on a response variable using semipartial R^2 (Legendre and Legendre, 2012). Largescale characteristics can be useful for denitrification prediction where they are indicative of broad functional attributes of the floodplain that integrate the multiple relationships of denitrification to its direct and local biogeochemical controls. The same variables used for path modeling were used for redundancy analyses; characteristics not statistically related to denitrification measurements were excluded to avoid artificially inflating adjusted R^2 values. Unique variation (the only statistically testable fraction) was tested for significance by permutation. Moderate to severe multi-collinearities (variance inflation factors $>$ 10) within each set of predictors were reduced by data reduction through principal component analysis. With the use of principal component scores as predictors, no severe multicollinearity (variance inflation factors $>$ 15) was found across the two sets of predictors. Path modeling was conducted in Mplus v7.11 (Muthén and Muthén, 2013). All other statistical analyses were conducted in R v3.3.2 (R Core Team, 2015). Statistical significance was defined at $\alpha = 0.05$.

3. Results

Data generated by this study are available at https://doi.org/10.5066/F7JW8D3W.

3.1. Variability in denitrification potentials and soil biogeochemical characteristics

The three denitrification potentials were measured either as enzyme activity (*i.e.*, with saturation and nutrient amendment), on unsaturated static cores at field moisture, or on saturated static cores with different nutrient amendments. Because of concern with nitrate limitation of denitrification during short-term incubations with unamended static cores, we first demonstrated with trials that N_2O production from saturated soil was constant (not limited by nitrate) over an 8-h incubation period from one of our sites with low soil N (Difficult Run, VA; Table 1 and Fig. 2). For the trials, linear rates in denitrification potential occurred for the 6 cores sampled at 2, 5, and 8 h (all $R^2 \geq 0.97$) while a decreasing rate occurred for another 6 soils sampled at 7, 11 and 23 h (R^2 ranged from 0.70–0.98).

Variability in the measurements of denitrification potential across all sites and sampling times was high (Fig. 4). Rates of DP_{DEA} in spring (7.2–1113 μg-N kg^{-1} h^{-1}) and summer (9.7–1192 μg-N kg^{-1} h^{-1}) consistently spanned 3 orders of magnitude. For DP_{FM} (May and August) and DP measurements on saturated static cores (July), variability also spanned 2–3 orders of magnitude, and DP_{FM} exhibited greater range in spring (0.1–166.4 μg-N m^{-3} h^{-1}) than summer (2–38.6 μg-N kg^{-1} h^{-1}). DP_{DEA} and DP_{FM} were moderately correlated in spring ($r = 0.70$, $P = 0.001$) and summer ($r = 0.49$, $P = 0.039$).

Season of sampling affected many of our repeated measurements. In summer, rates of DP_{FM} were lower than in spring ($t = -3.94$, $P = 0.001$), as were values of soil moisture ($t = -3.5$, $P = 0.002$), ammonium ($t = -10.8$, $P < 0.001$), and organic matter ($t = -4.05$, $P < 0.001$). At the same time, floodplains in summer had higher soil nitrate ($t = 5.94$, $P < 0.001$), SRP ($t = 7.05$, $P < 0.001$), pH ($t = 2.3$, $P = 0.035$) and temperature (22.9, $P < 0.001$). Date of sampling had no effect ($P > 0.05$) on DP_{DEA}, soil nutrient ratios, bulk density, C, and N. The remaining floodplain soil characteristics were measured only once.

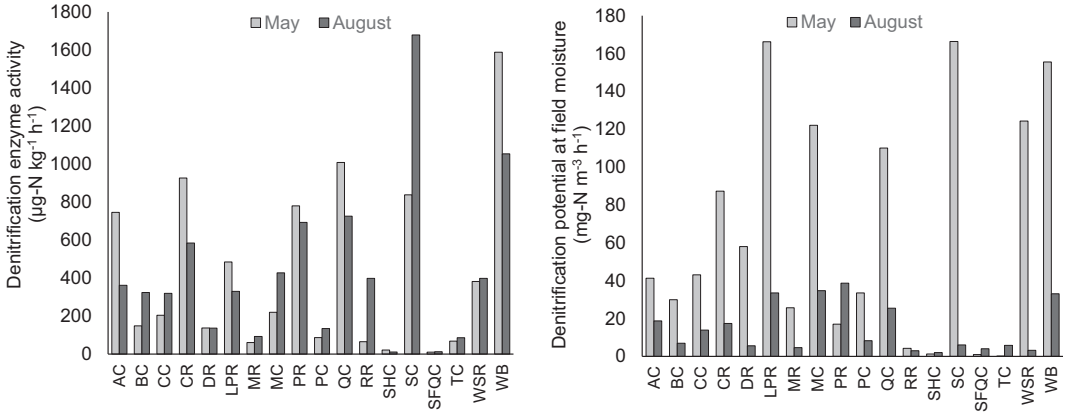

Fig. 4. Seasonal rates of DP_{DEA} (denitrification enzyme activity) measured on saturated and nutrient amended soils and DP_{FM} (denitrification potential at field moisture) measured on unsaturated and unamended soil. See Fig. 2 for site acronyms.

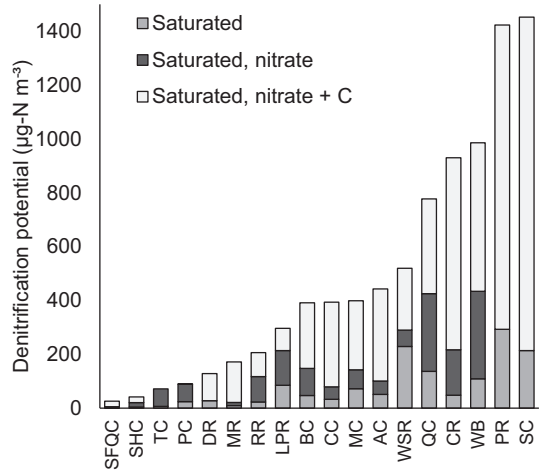

Fig. 5. Gains in DP_S with two nutrient amendments (= DP_{SN} and DP_{SNC}) in July. See Fig. 2 for site acronyms.

3.2. Relationships of local and largescale environmental characteristics with denitrification potentials

We inferred substrate limitation of denitrification potential for each site because mean rates of amended and saturated cores were larger in value (directionally) than the mean rates in unamended and saturated cores. Denitrification potential measured in saturated cores was limited by nitrate in 15 of 18 floodplains ($DP_{SN} > DP_S$), including solely by nitrate in one floodplain ($DP_{SNC} = DP_{SN}$); limited jointly by nitrate and C at 14 sites ($DP_{SNC} > DP_{SN} > DP_S$); and limited by a combination of nitrate and/or C at all sites ($DP_{SNC} > DP_S$) (Fig. 5).

One or more denitrification potentials (DP_{DEA} or DP_{FM} in spring or summer) were positively related to many local characteristics, namely soil pH, moisture, potential C mineralization, organic matter, C, N, P, C:N, nitrate, and SRP, and herbaceous AGB; DP_{FM} in August was negatively related to bulk density (Table 2). The adjustment of DP_{DEA} on a dry weight basis involved soil moisture and thus moisture was not assessed as a predictor of DP_{DEA} (Table 2). No denitrification potentials were related to mean maximum daily June or July soil temperature, soil ammonium, soil N:P or C:P ratios, herbaceous plant cover, belowground biomass, or the percent of silt and clay in the soil (Table 2).

The seven measurements of denitrification potential were linearly related to multiple largescale characteristics (Table 3): positive predictors of denitrification potential were floodplain sedimentation rates, stream total N and P concentrations, and catchment urban land cover; negative predictors were catchment forested land cover, seasonal daily maximum air temperature, and channel width-to-depth ratio (statistical test: linear regression with model fit by restricted maximum likelihood). For catchment land cover, DP_{DEA} decreased more gradually with % forested land cover than it increased with % urban land cover (Fig. 6). None of the seven measurements of denitrification potential were linearly related to channel or floodplain width, bank height, stream slope, stream discharge, stream elevation, catchment area, catchment agricultural land cover (Fig. 6), annual daily maximum air temperature, or physiographic province (Table 3).

3.3. Identifying hydrogeomorphic, catchment-scale and physical predictors of denitrification potential

We found multiple instances of correlation among the largescale predictors that were linearly related to denitrification potentials (Table 4). Because of the strong correlations (both $|r| > 0.83$, $P < 0.001$) between forested land cover and stream concentrations of N and P, and considering that nutrient inputs and nutrient exports can be higher in watersheds with greater proportion of non-forested land

Table 2
Regression coefficients for the linear relationships between floodplain soil and vegetation explanatory variables and denitrification potential response variables[1] by month of sampling.

Explanatory variables	DP_{DEA} (May)	DP_{DEA} (August)	DP_{FM} (May)	DP_{FM} (August)
Soil pH	0.46**	0.39**	21.9	0.55^{g}
Soil gravimetric moisture	na	na	114	29.7^{*r}
Soil bulk density	−0.49	−0.78	−45.4	-16.8^{*g}
Soil potential C mineralization	3.96**	nm	302*	nm
Soil organic matter	0.14*	0.19**	9.02	3.44^{***g}
Soil C	0.32*	0.29**	19.4	1.63^{r}
Soil N	5.32**	5.28**	340	76.8^{*s}
Soil P	1.37**	1.45***	64.9	7.94^{g}
Soil C:N	0.17^{***g}	0.04	8.10	0.40^{g}
Soil C:P	−0.10	−0.01	−1.99	0.08
Soil N:P	−1.86	−0.18	−59.7	2.69
Soil ammonium	0.05	0.17	34.6	8.86^{g}
Soil nitrate	1.03***	1.55***	80.8***	17.3^{*r}
Soil soluble reactive P	0.35*	2.01	7.84	3.36^{g}
Soil silt and clay	0.00	0.01	0.22	0.18^{r}
Herbaceous aboveground biomass	1.02	1.10*	96.3	3.97^{g}
Herbaceous plant cover	0.02	0.01	0.88	−0.04
Belowground biomass	−0.77	−0.71	−75.4	-1.53^{g}
June temperature, mean daily maximum	0.11	na	−0.50	na
July temperature, mean daily maximum	na	0.03	na	0.52

Notes: $*P < 0.05$; $**P < 0.01$; $***P < 0.001$.
Letters indicate the type of correlation structure applied to the model to eliminate spatial dependency in the residuals: g = Gaussian, r = rational, s = spherical.
Missing data acronyms: na = not applicable; nm = not measured.
[1]Denitrification enzyme activity (DP_{DEA}) is expressed as $\mu g\text{-}N\,kg^{-1}\,h^{-1}$ and denitrification potential measured at field moisture (DP_{FM}) is expressed as $\mu g\text{-}N\,m^{-3}\,h^{-1}$.

cover (Vogt et al., 2015), we inferred that catchment forested land cover (proportion of area) caused gradients in N and P stream concentrations and their positive effects on denitrification potential (Tables 3 & 4). To eliminate collinearity in further statistical tests, we used catchment forested land cover as a proxy for stream N and P concentrations. For the positive correlation between catchment forested land cover and spring air temperature (Table 4), we assessed whether the variables had unique effects (*i.e.*, effect controlling for another variable's effect) on spring DP_{DEA} and DP_{FM} apart from geographic overlap. With partial regression coefficients, only forested land cover was a significant predictor of spring DP_{DEA} ($b = -1.27$; $P = 0.023$) but not DP_{FM} ($b = -0.16$; $P = 0.135$). In other words, once the variation explained by forested land cover was accounted for, the remaining variation in spring DP_{DEA} ($b = -0.11$; $P = 0.209$) or DP_{FM} ($b = -0.66$; $P = 0.520$) explained by spring temperature was not significant. In summer, however, lower daily maximum air temperature predicted higher DP_S (Table 3) and was not correlated with forested land cover. We retained daily temperature as a predictor of DP_{DEA} in the spring for analyses of the third and fourth objectives, as explained below. The negative correlation between stream N concentration and spring air temperature was interpreted as an effect of catchment forested land cover and not assessed further (Table 4).

3.4. Mediating effects of floodplain soil and vegetation (local) predictors

We constructed path models with the predictors that were found to be significantly related to DP_{DEA} and DP_{FM} (*i.e.* Tables 2 and 3). Those predictors that had been modeled with spatial correlation structures could be included in the redundancy analysis because the spatial correlations were statistically explained using the largescale predictors: for spring DP_{DEA}, including either sedimentation or daily maximum spring temperature as a covariate in the regression model removed the

Table 3
Regression coefficients for the linear relationships between largescale explanatory variables and denitrification potential response variables[1] by month of sampling.

Largescale explanatory variables	DP_{DEA} (May)	DP_{DEA} (August)	DP_{FM} (May)	DP_{FM} (August)	DP_S (July)	DP_{SN} (July)	DP_{SNC} (July)
Channel bank height	0.27	0.33	12.3	-3.50[g]	0.17	0.19	0.25
Channel width	0.00	0.01	−1.80	−0.11[g]	−0.00	0.00	0.01
Channel width-to-depth ratio	−0.03	−0.04	−8.32**	−0.18[g]	−0.04	−0.03	−0.02
Entrenchment ratio	−0.05	−0.04	−2.61	0.35[d]	−0.04	−0.04	−0.06
Floodplain width	−0.00	−0.00	−0.36	−0.02[g]	−0.00	−0.00	−0.00
Stream slope	−85.4	−140	9660	1648[g]	34.1	−3.59	−67.7
Stream elevation	0.00	0.00	0.26	−0.01[g]	0.00	0.00	0.00
Stream discharge	0.31	0.33	−27.4	−1.66[g]	0.12	0.24	0.30
Stream total N concentration	0.89*	0.69*	45.0	7.20[g]	0.54	−0.56	0.56
Stream total P concentration	1.42**	1.13**	64.0	7.42[g]	0.78	0.76*	0.85
Floodplain sedimentation	0.00*	0.00*	0.01*	−0.00[g]	0.00	0.00	0.00
Catchment-scale forested land cover	−1.57**	−1.30*	−113*	−35.0**	−1.15*	−1.12*	−0.99*
Catchment-scale urban land cover	1.61*	0.98	161*	4.74[g]	1.38*	0.84	0.84
Catchment-scale agricultural land cover	0.63	0.78	18.2	19.4[g]	0.40	0.67	0.57
Catchment-scale drainage area	0.00	0.00	−0.05	−0.00[g]	0.00	0.00	0.00
Daily max. Air temperature, spring	−0.20*	n/a	−13.6	n/a	n/a	n/a	n/a
Daily max. Air temperature, summer	n/a	−0.19	n/a	−3.79[r]	−0.35*	−0.27	−0.27
Daily max. Air temperature, full year	−0.18	−0.11	−13.2	−1.68[g]	−0.16	−0.14	−0.15
Physiographic province[2]	0.39	0.17	0.19	1.10	0.73	0.83	0.46

Notes: *$P < 0.05$; **$P < 0.01$; ***$P < 0.001$.
Letters indicate the type of correlation structure applied to the model to remove spatial dependency in the residuals: g = Gaussian, r = rational, s = spherical.
[1]ANOVA *F* values presented for physiographic province.
[2]Denitrification enzyme activity (DP_{DEA}) is expressed as μg-N kg^{-1} h^{-1} and denitrification potential measured at field moisture (DP_{FM}) is expressed as μg-N m^{-3} h^{-1}.

significant spatial correlation with C:N; for summer DP_{FM}, including forested land cover in the regression model removed the significant spatial correlations with moisture, bulk density, organic matter, N, and nitrate. Daily temperature, though not a predictor of denitrification potential after controlling for forested land cover, was used as a statistical control to derive the unique variability explained by forested land cover.

Path modeling revealed a plausible set of explanatory mechanisms (indirect pathways) for the (direct) effects of largescale characteristics on DP_{DEA} and DP_{FM} (Tables 5 and 6). Catchment forested land cover had direct partial effects on DP_{DEA} (paths A; Fig. 3) in spring and summer, and floodplain soil nitrate, soil P, and AGB were mediators of these relationships (AGB in summer): partial correlation between DP_{DEA} and soil nitrate, soil P, and AGB were significant (paths D), as were the effects of forested land cover on soil nitrate, soil P, and AGB (paths B) (Table 5). Thus, greater non-forested land cover promoted greater soil DP_{DEA}, nitrate, P, and AGB in floodplains, and separate from these effects, DP_{DEA} positively tracked with nitrate, P, and AGB in floodplain soils. In spring and summer, floodplain sedimentation also had a direct partial effect on DP_{DEA} at the same time that sedimentation had an effect on soil P, pH, and potential C mineralization, which in turn were all partially correlated (positively) with DP_{DEA} (Table 5). On DP_{FM},

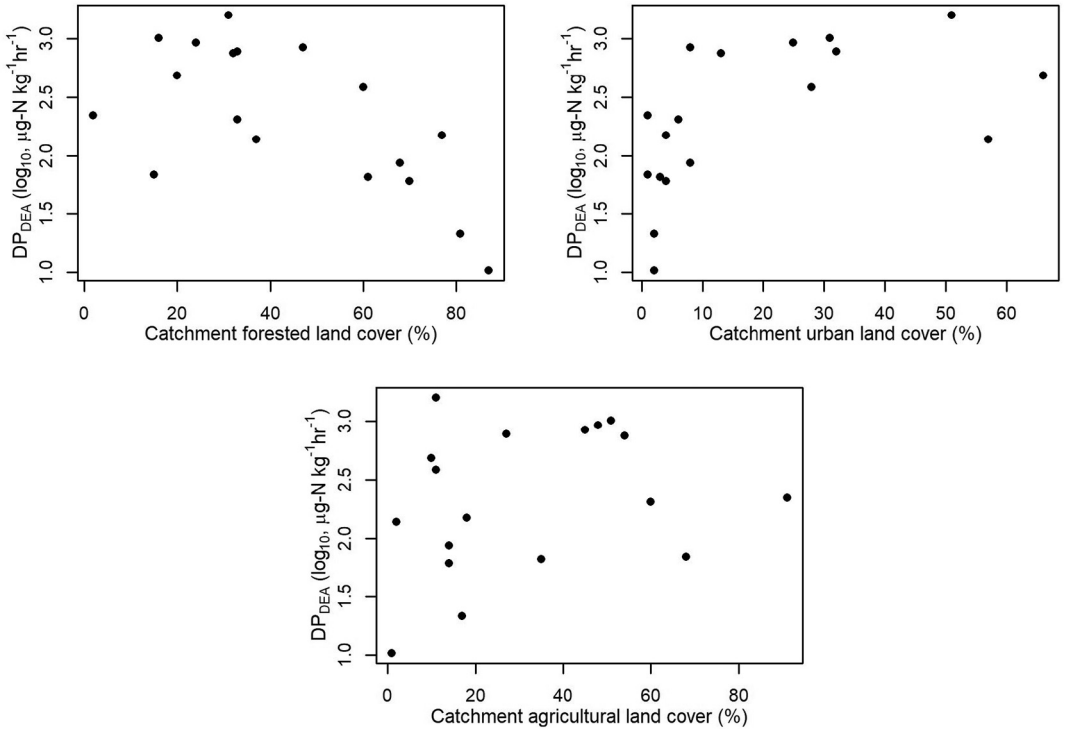

Fig. 6. Scatterplots of catchment land cover with denitrification enzyme activity (DP_{DEA}) in spring.

Table 4
Correlation matrix for hydrogeomorphic, catchment-scale, and climate predictors[1] of denitrification potentials.

	Forest	Urban	Stream N	Stream P	Channel WD	Sediment.	Air Temp. Spring
Urban	x						
Stream N	−0.84***	x					
Stream P	−0.83***	x	0.78***				
Channel WD	0.4†	x	x	x			
Sediment.	x	x	x	x	x		
Air Temp. Spring	0.48*	x	−0.59**	x	x	x	
Air Temp. Summer	x	x	−0.44†	x	x	x	0.86**

Notes: Notation of statistical significance: x denotes $P > 0.1$; †$P < 0.1$; *$P < 0.05$; **$P < 0.01$; ***$P < 0.001$.
Abbreviations: Forest = catchment forested land cover, urban = catchment urban land cover, stream N = stream N concentration, stream P = stream P concentration, WD = width-to-depth ratio, sediment. = floodplain sedimentation, air temp. = maximum daily air temperature.
[1]Predictors are characteristics that are linearly related to at least one denitrification potential (Table 3).

catchment forested land cover, floodplain sedimentation, and channel width-to-depth ratio had significant partial effects in spring and or summer (Table 6). DP_{FM} was positively and partially correlated to potential C mineralization in the spring, and both variables were affected by floodplain sedimentation.

3.5. Partitioning explained variation among local and largescale predictors

Using redundancy analysis, we partitioned variation of each May and August denitrification potential measurement between floodplain soil and vegetation (local) predictors and hydrogeomorphic, catchment-scale, and physical (largescale) predictors (Fig. 7). The same predictors used for path modeling were used for redundancy analysis. Given the evidence in summer for air temperature's relationship to denitrification, we assigned the shared variability between daily temperature and forested land cover to daily temperature and thus included both predictors (both now statistically significant) in the spring model for DP_{DEA}. Within the set of local predictors, we reduced severe collinearity using principal component scores that captured the bulk percentage of total variation between the variables: soil potential C mineralization, organic matter, C, and N in spring (91%); soil organic matter, C, and N in the summer for DP_{DEA} (95%) or soil organic matter and N in summer for DP_{FM} (97%); and soil pH and SRP in spring (92%). Largescale predictors explained 43–57% of variation in denitrification potentials (unique and shared variation with the local predictors), with 22–30% of DP_{FM} uniquely explained ($P < 0.05$) in spring and summer (Fig. 7). Floodplain soil and vegetation predictors explained between 27 and 77%, with 15% of DP_{DEA} uniquely explained ($P < 0.05$) in spring (Fig. 7). Shared variation between the largescale and floodplain soil and vegetation predictors ranged from 15 to 46% (not statistically testable), while unexplained variation was greater in the summer (41–43%) than spring (13–32%) (Fig. 7).

4. Discussion

4.1. Variability in denitrification potential related to local characteristics across sites

Variability in denitrification potential (*i.e.*, DP_{DEA} or DP_{FM}) followed a suite of local floodplain soil and vegetation characteristics (12 total), in summary of results for our first objective. Because we assessed interactions between soil biogeochemistry, soil composition and formation, and the vegetation community as influenced by hydrogeomorphic processes in floodplains and regional scale environmental heterogeneity

Table 5
Standardized coefficients from path models (Fig. 3) for partial effects of largescale predictors[1] on denitrification enzyme activity (DP_{DEA}) (path A) and an individually-modelled[2] floodplain local predictor[3] (Paths B or C)[4], and resulting partial correlation between DP_{DEA} and the local predictor (Path D), with emphasis (underline) given to paths within a model (composite of paths A, B/C, and D) that reveal a plausible mechanism for the direct effect of a largescale characteristic on DP_{DEA}.

Largescale predictors[5]	Path A: DP_{DEA}	Paths B,C,D	Nitrate	SRP	P	pH	Pot. C min.	Organic matter	C	N	C:N	AGB
Spring												
1. Floodplain sedimentation	0.36*	B:	0.28	0.26	0.00*	0.40*	0.53**	0.26	0.21	0.30	−0.07	n/a
		D:	0.71***	0.72***	0.03*	0.66***	0.59***	0.65***	0.68***	0.72***	0.44*	
2. Catchment forested land cover	−0.43**	B:	−0.45**	−0.19	−0.98***	−0.23	−0.08	−0.06	−0.03	0.01	−0.15	n/a
		D:	0.71***	0.72***	0.03*	0.66***	−0.59***	0.65***	0.68***	0.72***	0.44*	
3. Catchment urban land cover	0.19	B:	−0.02	−0.54**	−0.62**	−0.33	−0.25	0.08	0.00	−0.01	0.10	n/a
		D:	0.71***	0.72***	0.03*	0.66***	−0.59***	0.65***	0.68***	0.72***	0.44*	
4. Daily maximum spring air temperature	−0.20	B:	−0.34	−0.48***	−0.00	−0.55**	−0.27	−0.03	−0.18	−0.17	0.05	n/a
		D:	0.71***	0.72***	0.03*	0.66***	−0.59***	0.65***	0.68***	0.72***	0.44*	
Summer												
5. Floodplain sedimentation	0.42**	B/C:	0.33	n/a	0.19	0.32	n/a	0.27	0.30	0.33	n/a	0.03
		D:	0.57***		0.52**	0.56**		0.67***	0.53**	0.61***		0.39*
6. Catchment forested land cover	−0.51**	B:	−0.53**	n/a	−0.69***	−0.31	n/a	−0.21	−0.22	−0.26	n/a	−0.42*
		D:	0.57***		0.52**	0.56**		0.67***	0.53**	0.61***		0.39*

Notes: *$P < 0.05$; **$P < 0.01$; ***$P < 0.001$.
[1]Variables linearly related to DP_{DEA} in either spring or summer (Tables 2 and 3) were modeled, otherwise "n/a".
[2]The spring and summer models were applied to each floodplain soil and vegetation predictor individually.
[3]All floodplain soil and plant predictors were measured seasonally with the exception of AGB and P. Abbreviations: SRP = soluble reactive phosphorus, Pot. C min. = potential carbon mineralization, AGB = herbaceous aboveground biomass.
[4]The path between floodplain sedimentation and herbaceous AGB (Path C) was modeled as a reciprocal effect (partial correlation).
[5]The following paths modeled between largescale predictors were statistically significant ($P < 0.05$): 2–3 (−) and 2–4 (+).

Table 6
Standardized coefficients from path models (Fig. 3) for effects of largescale predictors[1] on denitrification potential measured at field moisture (DP_{FM}) (Paths A) and an individually-modelled[2] floodplain soil predictor (Paths B)[3] and resulting partial correlation between DP_{FM} and the soil predictor (Path D), with emphasis (underline) given to paths within a model (composite of paths A, B/C, and D) that reveal a plausible mechanism for the direct effect of a largescale characteristic on DP_{FM}.

Largescale predictors[4]	Path A: DP_{FM}	Path	Nitrate	Pot. C min.	Organic matter	N	Grav. moisture	Bulk density
Spring								
1. Floodplain sedimentation	0.30*	B:	0.27	0.54**	n/a	n/a	n/a	n/a
		D:	0.58***	0.42**				
2. Channel width-to-depth ratio	−0.39*	B:	−0.05	0.04	n/a	n/a	n/a	n/a
		D:	0.58***	0.42***				
3. Catchment forested land cover	−0.17	B:	−0.58**	−0.21	n/a	n/a	n/a	n/a
		D:	0.58***	0.42***				
4. Catchment urban land cover	0.29	B:	0.04	−0.20	n/a	n/a	n/a	n/a
		D:	0.58***	0.42***				
Summer								
5. Catchment forested land cover	−0.70***	B:	−0.57***	n/a	−0.25	−0.30	−0.29	−0.16
		D:	0.30		0.45*	0.22	0.65***	−0.53**

Notes: $*P < 0.05$; $**P < 0.01$; $***P < 0.001$.
[1]Variables linearly related to DP_{FM} in either spring or summer (Tables 2 and 3) were modeled, otherwise "n/a".
[2]The spring and summer models were applied to each floodplain soil and vegetation predictor individually.
[3]All floodplain soil and plant predictors were measured seasonally. Abbreviations: Pot. C min. = potential carbon mineralization; Grav. moisture = gravimetric moisture.
[4]The following relationships between largescale predictors were statistically significant ($P < 0.05$): 3–4 (−).

of the Chesapeake Bay watershed (Fig. 1), we discuss the local predictors of our denitrification potentials in the context of largescale characteristics below. We had expected that denitrification potential variability would most strongly follow the direct controls on the denitrification process (*i.e.*, nitrate, organic C, oxygen, pH, and temperature of soil). Following those expectations, we found that N and C-related soil floodplain characteristics (*i.e.*, nitrate, N, organic matter, Pot. C. min, C:N), were in aggregate the most consistent predictors (all positive) of DP_{DEA} and/or DP_{FM}.

Results from our substrate limitation measurements of denitrification potential (DP_S, DP_{SN}, and DP_{SNC}) provided experimental corroboration for the strong control exerted by nitrate and organic C. Using saturated soil cores, the experiment demonstrated that floodplains were largely limited by either nitrate or combined nitrate and C. Only in

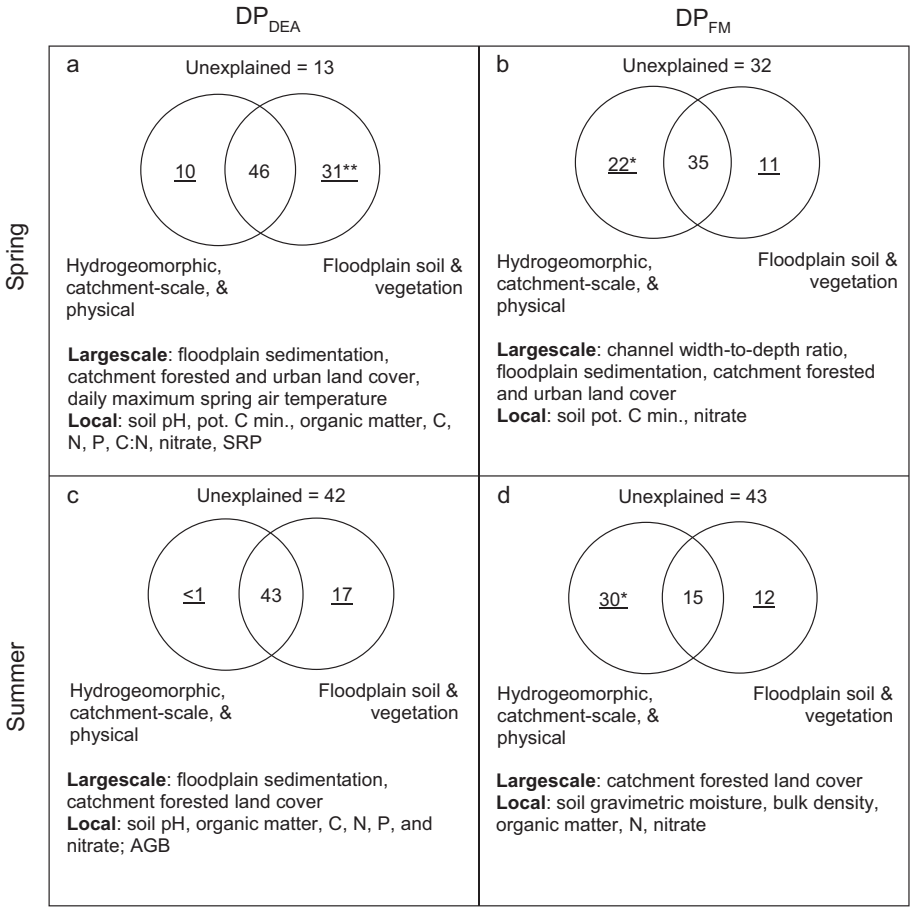

Fig. 7. Partitioned percent variation of DP_{DEA} and DP_{FM} variables for May and August by largescale (*e.g.*, hydrogeomorphic) and local (*e.g.*, soil) predictors. Unexplained percent variation outside circles. Underlined values are statistically testable, non-shared fractions: $*P < 0.05$; $**P < 0.01$; $***P < 0.001$. Abbreviations: Pot. C min. = potential carbon mineralization, SRP = soluble reactive phosphorus, AGB = herbaceous aboveground biomass.

three floodplains (all with catchments high in either agricultural or urban land cover) was denitrification potential not limited by nitrate. Of those exhibiting nitrate limitation, two floodplains were almost entirely limited by nitrate (relative to C limitation) that were both on the Coastal Plain with sandy soils and high entrenchment ratios (> 8). One of these floodplains, Tuckahoe Creek, showed little soil development with the lowest soil C, N, organic matter, potential C mineralization, C:P, N:P, and moisture, and the highest soil bulk density, across seasons. The other floodplain, Polecat Creek, was notable for the highest belowground biomass (and below-average organic matter and nutrient stores). Thus, almost-singular nitrate limitation was linked to both low nutrient soils as well as soils inferred to have large soil C inputs from belowground biomass. Most floodplains (14 of 18) showed both nitrate ($DP_S < DP_{SN}$) and C limitation ($DP_{SN} < DP_{SNC}$), indicating predominantly joint regulation at regional scales. While this study did not examine isolated C limitation (in the absence of nitrate amendment), our measurements provide evidence that denitrification potential varied considerably with C where/when nitrate demand had been met. Waters et al. (2014) found that denitrification potential was primarily C limited in some forested and especially herbaceous riparian soils in urban catchments near Baltimore, MD. Relationships of DP_{DEA} and DP_{FM} with microbial respiration, an index of labile C availability, and the soil C:N ratio, also implicates C limitation.

Large environmental changes in the Chesapeake Bay watershed from spring to summer were expected to influence floodplain denitrification. Stream baseflow was substantially lower in August than May at all sites. Herbaceous vegetation had also grown thicker and taller by August (and exceeded 2 m in height at Quittapahilla Creek). Indeed, we found widespread variability in our repeated measurements of denitrification potential, floodplain nutrient availability, and of the strength of relationships between denitrification with local and largescale characteristics. Average DP_{FM} was lower in the summer, concurrent with lower soil moisture, ammonium, and organic matter; and higher soil temperatures, nitrate, SRP, and pH. Denitrification responds exponentially to changes in water-filled pore space within a threshold of 60–80% (Machefert and Dise, 2004), and median water-filled pore space dropped from spring (75%) to summer (64%). Two soil characteristics measured in both May and August, SRP and C:N, were (positive) predictors only in spring. Wetter soils in May would have stimulated potential C mineralization (Wilson et al., 2011; Shrestha et al., 2014), and C demand in turn would have increased the importance of soil C:N. By summer, soil organic matter stores were smaller and labile C pools may also have more evenly inhibited denitrification across sites (weakening denitrification potential – C:N relationships). Senescence of ephemeral spring vegetation was first observed in July, and thus increases in water-soluble labile C from the senescence of spring vegetation were less likely to have contributed to the results in May. For SRP, lower availability in spring would strengthen the relationship to DP_{DEA}.

4.2. Influence of largescale characteristics on denitrification potential

Channel dimensions can be useful indicators of difficult to measure hydrologic and geomorphic processes (Schenk et al., 2013). In the spring, small width-to-depth ratio of stream channels (more incised or constrained) was a linear predictor of high DP_{FM}, with direct but no mediating effects on DP_{FM} identified (path modeling). One explanation for the relationship with denitrification potential is that lower riparian water table levels in constrained streams increases soil oxygenation and production of nitrate through nitrification (Groffman et al., 2002). Alternatively, spring flooding can export inorganic N and P from floodplains, and particularly nitrate, a primary predictor of denitrification potentials in spring (Noe and Hupp, 2007). Greater channel width-to-depth ratio was associated with lower annual stream flow ($r = 0.54$, $P = 0.020$) and smaller drainage area, with three of the five lowest ratios found in the smallest catchments (21.7–32.7 km^2), with possible implications for denitrification. Greater channel width is associated with greater annual peak bankfull discharges (Parrett and Johnson, 2004), and for floodplains in the Chesapeake Bay watershed, likely more frequent or energetic spring flooding with higher winter and spring baseflow. Both explanations of the response of soil nitrate levels to degree of saturation or flooding would explain why channel width-to-depth ratio was only inversely associated with DP_{FM}: a measurement of denitrification potential in field moist, whole soil cores that shows sensitivity towards short-term fluctuations in the substrate controls on the process (*e.g.*, nitrate). Catchment drainage area was not predictive of denitrification, in contrast to other studies that have found changes in floodplain biogeochemistry along longitudinal gradients of streams from headwaters to larger rivers (Arp and Cooper, 2004; Noe et al., 2013).

Though water fluctuations in floodplains leach short-term mineralized nutrient forms (Bechtold et al., 2003), greater hydrologic connectivity between the stream and floodplain increases accumulation of soil, organic material and dissolved nutrient inputs from sedimentation (Steiger and Gurnell, 2002; Noe and Hupp, 2005; Wolf et al., 2013). Sedimentation may also be a better indicator of hydrologic connectivity than steam-channel geometry at regional scales, as sedimentation was the only largescale predictor correlated with floodplain soil moisture (summer: $r = 0.59$, $P = 0.011$). For this study, our measurement of sedimentation captured a long-term soil-building influence - as mass accumulation over a mean of 45 years. Both nutrient deposition and dissolved inputs, in turn, can have large influences on floodplain biogeochemical cycling (Wassen and OldeVenterink, 2006; Noe et al., 2013; McMillan and Noe, 2017). Because floodplain sedimentation related positively to DP_{DEA} and DP_{FM}, and specifically to DP_{DEA} across seasons, our data indicated that sedimentation was an important control on denitrification potential at regional scales. McMillan and Noe (2017) reported that variability in mass of nutrient deposition to floodplains was predominantly driven by rates of sedimentation, and that both were predictors of floodplain denitrification. We thus attribute the effect of sedimentation on denitrification potential in part to greater hydrologic connectivity that led to greater nutrient (*e.g.*, N, C, or P) deposition, and the stimulation of floodplain soil biogeochemistry as a result. In support of this conclusion, variability of sedimentation across the Chesapeake Bay watershed reflects a strong legacy of land use change and agriculture, where highest yields of channel suspended sediment are linked to agricultural land use (Langland and Cronin, 2003; Gellis et al., 2009), which suggests dually high nutrient loading to floodplains.

Our path models identified greater soil P, pH, and potential C mineralization as explanations for the effect of sedimentation on denitrification potential in the spring. Though no directional relationship was defined in the path models between denitrification potential and the local predictors, predominantly unidirectional effects best explain the observed relationships as discussed below. This study and others have found that denitrification rates and potentials positively track with levels of floodplain P (Ashby et al., 1998; McMillan and Noe, 2017), the relative availability of which can limit general nutrient processing in floodplains (Schilling and Lockaby, 2005). Floodplains sequester large quantities of P from streams, which is largely in particulate form adsorbed to sediment, and they can serve as sinks for SRP during flooding. Compared to all sources of floodplain P (*e.g.*, overland or subsurface flow), flood deposition of particulate P contributes the most towards floodplain P retention (Noe and Hupp, 2007; Hoffman et al., 2009). Denitrification also responds strongly to soil pH levels; eight sites had pH within 6–8, an optimal range for the process, while three sites had a pH below 5 at which severe limitation of denitrification occurs (Saleh-Lakaha et al., 2009). Both P and pH have been found to be positively related to each other in floodplains and to zones of the floodplain receiving the greatest sedimentation (Kaase and Kupfer, 2016). The higher concentrations of nutrients (*e.g.*, base cations) that accompany high rates of sedimentation, as well as labile organic matter and greater

hydrologic connectivity, might buffer soil pH levels from long-term microbial decomposition of organic matter and would raise potential C mineralization with greater labile C stores (*e.g.*, dissolved organic C) (Reddy and DeLaune, 2008). Thus, the positive associations between denitrification measurements, potential C mineralization, and pH, as affected by floodplain sedimentation, suggests that pH is positively affected by greater microbial heterotrophic respiration generally, of which denitrification contributes a small part (Megonigal and Neubauer, 2009). Our measurement of potential C mineralization was taken on field moist soils and captures microbial respiration as affected by site moisture levels. The positive effect of floodplain sedimentation on both spring DP_{DEA} and DP_{FM} through the index of labile C could have been due to a contributing effect of greater soil moisture promoting short-term microbial decomposition (Wilson et al., 2011).

Catchment forested land cover was a consistent predictor of the seven measurements of denitrification potential (*i.e.*, enzyme activity and potentials, in unsaturated and saturated cores, in spring and/or summer). For six of those measurements, denitrification potentials were markedly elevated in catchments with < 60–80% forested land cover; for the summer measurements of DP_{FM}, marked increases were in catchments with < 60% forested cover. Because forested and agricultural land cover were inversely, linearly related ($r = -0.66$; $P = 0.003$), but forested and urban land cover were not, the largest contributor to control of denitrification by forested land cover came from agricultural land use (although agricultural land cover was not itself directly related to denitrification potentials). The path models identified soil nitrate, soil P, and herbaceous AGB as positive mediators of the causal effect of forested land cover on DP_{DEA}; we infer predominantly unidirectional relationships between these three local predictors and DP_{DEA} as discussed below. McMillan and Noe (2017) found that dissolved input of nitrate to floodplain soils, from overbank flooding and overland flow, was positively related to denitrification, and its spatial gradients across floodplains partially differed from sedimentation patterns. In the same way, the positive effect on soil P in non-forested catchments, which was separate from the effect of sedimentation, likely included P from overland flow and dissolved P in floodwater. The two sites (Sideling Hill Creek and South Fork Quantico Creek) with the highest percent of catchment forested land cover and consistently very low DP_{DEA} and DP_{FM} rates also had the two lowest concentrations of soil total P. Anthropogenic land use has previously been linked to reduced N limitation of plants and greater soil P levels in floodplains (Antheunisse et al., 2006). Greater nitrate and soil P likely promoted a larger and more diverse herbaceous vegetation community (herbaceous cover ranged from 41 to 97%) which could favor denitrification potentials such as from greater inputs of labile C to the soil (*e.g.*, Korol et al., 2016).

Isolating the individual effects of urban or agricultural land cover type presents analytical challenges for inherently covarying land cover classes. The strong inverse relations of our denitrification potentials with forested land cover in the Chesapeake Bay watershed make intuitive sense as both urban and agricultural land cover are both large sources of anthropogenic nutrients to the Bay (Ator et al., 2011). Furthermore, catchments with high urban and agricultural land cover overlap spatially at a regional scale in the Chesapeake Bay watershed, with high stream nutrient concentrations in the north and east, while greater forested land cover and lower stream nutrients are found to the south and west (Langland et al., 2013). As a result, below-average denitrification potentials across the seven measurements were consistently found at the four sites in southern Virginia with catchment forested land cover ≥61%. At the same time, the lack of linear relationships of agricultural land cover with denitrification potentials were still surprising. In the Chesapeake Bay watershed, Waters et al. (2014) found that denitrification potentials in forested floodplains of a highly agricultural catchment (57%) were higher than potentials in either highly urban or forested catchments (equivalent potential rates) all located around Baltimore, MD at landscape scale (*i.e.*, < 50 km). Two sites in catchments with the highest percent agricultural land cover (≥ 68%) in this study (neither with notably high denitrification potentials, and one with below-average denitrification potentials) were located on the Eastern Shore (the Delmarva Peninsula), which exhibits nationally high rates of N and P inputs to catchments and surface- and groundwater (Denver et al., 2004). However, dense agricultural land cover is not unique to the Coastal Plain, and greater variability in agriculture's influence on denitrification potential might be due to the confounding influence of largescale hydrogeomorphic variability (*e.g.*, Hopkins et al., 2015) found across the watershed (*e.g.*, entrenchment ratios, though not predictive of denitrification potentials, were strongly related to physiographic location in the watershed); five catchments with percent agricultural land cover between 45 and 60% were scattered throughout the northern, central and western span of this study. This distribution of agriculture differs from more geographically clustered urban land use. Notably, low sediment yields in streams are found in heavily forested catchments and those of flat topography on the Eastern Shore (Langland et al., 2013), which would reduce sediment exchange between streams and floodplains. A second reason for the lack of relationships (or weak relationships undetectable by the sample size in this study) may have been due to the confounding influences of urban land cover on the percentage classes of agricultural land cover.

Urban land cover was a positive predictor of measured denitrification potentials (*i.e.*, DP_{DEA}, DP_{FM}, and DP_S) in the spring and early summer (July). In the Chesapeake Bay watershed, urban riparian wetlands serve as substantial sinks for nitrate mainly through denitrification, equivalent to between 8 and 11% of the daily nitrate loads in streams (Harrison et al., 2011). Our results differ from previous studies of floodplains conducted across smaller sub-regions of the Chesapeake Bay (*i.e.*, near Baltimore, MD) that found similar denitrification rates or potentials in urban and forested or rural catchments (Groffman and Crawford, 2003; Harrison et al., 2011; Waters et al., 2014). When modeled with other largescale predictors, catchment urban land cover had unique negative effects on soil P and SRP only (and not on the denitrification potentials). Hogan and Walbridge (2007) found depressed soil P levels and lower P sorption capacities in floodplains in highly urbanized watersheds (*i.e.*, 24.8–37.6% impervious surface cover), compared to moderately urbanized watersheds, attributable to hydrologic modification and deposition of crystalline Fe. By this standard, seven of the eighteen sites of this study were located in 'high' or 'very high' urbanized catchments (25–66%) and would have been susceptible to habitat modifications inhibiting P accumulation. Further resolution of urban and agricultural land cover (*e.g.*, with focus on spatial arrangement of cover in a catchment, or indices of stream-floodplain integrity) would likely better discriminate land cover effects on denitrification in floodplains. Denitrification potentials were consistently elevated at and above roughly 10% urban land cover (*e.g.*, Fig. 6), with pronounced lower rates at lower % urban cover, which indicates very little urban land cover of catchments can have large effects on floodplain denitrification.

Two spring and early summer denitrification potentials (*i.e.*, May DP_{DEA} and July DP_S) were inversely related to the maximum daily air temperature summarized by season (spring and summer). Daily maximum temperatures in May (20.4–22.1 °C) across all sites were slightly more variable than in July (30.6–31.9 °C). Warmer temperatures increase rates of microbial activity, microbial decomposition of organic matter, mineralization of organic N and P, and are associated with lower pools of labile organic C (Keddy and DeLaune, 2008), the latter of which would explain our results. An index of labile C was an important positive predictor of denitrification in the spring (related to both denitrification measurements). Highest denitrification rates were also found at intermediate soil temperatures (15–20 °C) in a largescale study of alluvial soils across Europe (Pinay et al., 2007). No partial effects of spring temperature on DP_{DEA} were found for the spring path models, presumably due to its shared variance with catchment forested land cover, but spring temperature did have negative effects on soil SRP and

pH in the models. Greater microbial activity that depletes organic matter stores with warmer temperatures would increase soil acidity. Greater statistical power might be necessary to resolve the separate mediating effects of spatially-dependent climate metrics and land cover on denitrification.

4.3. Partitioning variation among local and largescale predictors of denitrification potential

Local biogeochemical and vegetation controls are known to explain large portions of variability in denitrification, but their relationships at broad scales may change and not be as useful or practical as a predictive tool as those controls of denitrification having spatial interactions over larger scales (Merrill and Benning, 2006; Kulkarni et al., 2014). Our redundancy analysis results indicated that the soil and vegetation predictors explained a larger portion of variability in DP_{DEA} and DP_{FM} (up to 77%) compared to the hydrogeomorphic, catchment-scale, and climate predictors (up to 57%). In the spring, floodplain soil predictors also explained unique variation in DP_{DEA} and DP_{FM} not explained by the largescale predictors. Even so, the 43–57% of variation explained by the largescale predictors represents roughly half the variation in the two denitrification potentials that should be useful for prediction of denitrification across the Chesapeake Bay watershed. Largescale predictors explained unique variation only for the two DP_{FM} measurements (variation not explained by local predictors), which were related to fewer soil and vegetation characteristics than DP_{DEA}; only DP_{DEA} was positively related to soil P, SRP, pH, C, C:N, and AGB, suggesting these soil characteristics might be contributing variation to DP_{FM} (a measure of the short-term ability to denitrification) that was better (uniquely) explained by the largescale predictors. Merrill and Benning (2006) found that variation in denitrification potential was better explained by riparian ecosystem type, an integrated largescale predictor, then by soil physicochemical properties across a catchment. Progress in denitrification prediction will likely be made when denitrification's local controls are also linked to hydrogeomorphic characteristics and largescale characteristics of river catchments, enabling prediction of denitrification using existing largescale geospatial data.

5. Concluding remarks and implications

The need to understand patterns in denitrification, an important ecological function at regional scales, will continue to grow with the implementation of watershed N management. Many environmental characteristics should in theory relate to denitrification but are scale dependent (*e.g.*, variability often increases with physical distance) and have not been empirically tested across catchments that markedly differ in physiographic features. Because of the short-term and long-term drivers of denitrification, we used complementary measurement methods (*i.e.*, saturated *vs.* field moist soils, and substrate *vs.* no substrate amendment) of denitrification potential in our investigation (with a total of seven measurements across spring and summer). For prediction purposes at regional scale, the combined largescale predictors could explain up to a majority of variation (43–57%) in the denitrification measurements, which additionally offer more utility for practical application with publicly available datasets than floodplain soil or vegetation characteristics. Of the largescale characteristics, catchment forested land cover was the most consistent predictor (negatively) of all seven measurements of denitrification potential, while catchment urban land cover and floodplain sedimentation were the next two most consistent predictors (both positively) of denitrification metrics either in one or the other season. Mechanisms for the interaction of these largescale characteristics with denitrification were then explored using path models. Because the effects of catchment-scale forested land cover (negatively related to agricultural land cover and positively related to stream N and P concentrations) and floodplain sedimentation (likely also positively indicative of floodplain soil redox fluctuations) were related to important direct biogeochemical drivers (*i.e.,* soil N and C availability and pH) of denitrification among other influential indirect drivers (*e.g.*, soil P), hotspots of floodplain denitrification should be found in catchments of high non-forested land cover and reaches with high rates of nutrient sedimentation. Thus, floodplains in agricultural and urban catchments of the Chesapeake Bay watershed are removing more nitrate from streams that have greater stream N loads than more forested catchments.

For restoration purposes, increasing stream connection and promoting nutrient sedimentation to floodplains in urban or agricultural catchments – current areas prioritized for nutrient reduction, along with point sources – should remove more excess total N through denitrification (as well as N and P storage). This study provides evidence that the floodplains in these catchments are better at nitrate removal through denitrification predominantly because their location allows them to intercept more nutrients and sediments from their catchment and not because of marked locational differences in internal biogeochemical processing. Because all of the floodplains in this study were active and received floodwater regularly (though net sedimentation at the Warm Springs Run site was zero), the floodplains are reasonably representative of restored, re-connected floodplains that have elevated biogeochemical cycling from greater openness to material and energy inputs. Where restoration occurs to increase connectivity and stability, the restructured floodplains will still be subjected to regional-scale heterogeneity in catchment land cover patterns and sedimentation. That land cover or sedimentation were predominantly statistically linked to denitrification potential through changes to soil nutrient stores or indicators of nutrient availability, and not to soil structure, indicates that nutrient inputs promote denitrification through greater floodplain biogeochemical processing across soil types. Our conclusions apply best to large, regional gradients in nutrient delivery; at landscape scales ($\leq$100 km), largescale predictors may not strongly explain variability in nutrient loading or denitrification in floodplains where the strength of relationships of largescale and local characteristics may differ from this study.

Acknowledgements

Funding for this study was provided by the USGS Chesapeake Science Program, USGS National Research Program, Cosmos Club Foundation, Provost's Office at GMU, the Society of Wetland Scientists, and the South Atlantic Chapter of the Society of Wetland Scientists. Thank you to Cliff Hupp, Peter Claggett, Jaimie Gillespie, Mike Doughten, Tracie Spencer, Natalie Hall, Mario Martin-Alciati, Ricky Furusawa, Anthony Doane, Roslyn Cress, and Kelly Floro for your field, laboratory, and modeling contributions. Any use of trade, firm, or product names is for descriptive purposes only and does not imply endorsement by the U.S. Government.

References

Allan, J.D., 2004. Landscapes and riverscapes: the influence of land use on stream ecosystems. Annu. Rev. Ecol. Evol. Syst. 35, 257–284.

Antheunisse, A.M., Loeb, R., Lamers, L.P.M., Verhoeven, J.T.A., 2006. Regional differences in nutrient limitation in floodplains of selected European rivers: implications for rehabilitation of characteristic floodplain vegetation. River Res. Appl. 22, 1039–1055.

Arp, C.D., Cooper, D.J., 2004. Analysis of sediment retention in western riverine wetlands: the Yampa River watershed, Colorado USA. Environ. Manag. 33 (3), 318–330.

Ashby, J.A., Bowden, W.B., Murdoch, P.S., 1998. Controls on denitrification in riparian soils in headwater catchments of a hardwood forest in the Catskill Mountains, U.S.A. Soil Biol. Biochem. 30 (7), 853–864.

Ator, S.W., Brakebill, J.W., Blomquist, J.D., 2011. Sources, fate, and transport of nitrogen and phosphorus in the Chesapeake Bay watershed: an empirical model. In: U.S. Geological Survey. Scientific Investigations Report, pp. 2011–5167.

Bachman, L.J., Lindsey, B., Brakebill, J., Powars, D.S., 1998. Ground-water discharge and base-flow nitrate loads of nontidal streams, and their relation to a hydrogeomorphic classification of the Chesapeake Bay watershed, Middle Atlantic Coast. In: U.S. Geological Survey. Water-Resources Investigation Report, pp. 98–4059.

Bailey, R.G., 2009. Ecosystem Geography: From Ecoregions to Sites, Second edition.

Springer, New York, NY.
Bechtold, J.S., Edwards, R.T., Naiman, R.J., 2003. Biotic versus hydrologic control over seasonal nitrate leaching in a floodplain forest. Biogeochemistry 63 (1), 53–71.
Berg, J., et al., 2014. Recommendations of the Expert Panel to Define Removal Rates for Individual Stream Restoration Projects. Chesapeake Bay Program. http://www.chesapeakebay.net/publications/.
Bernard-Jannin, L., Sun, X., Teissier, S., Savage, S., Sánchez-Pérez, J.M., 2017. Spatio-temporal analysis of factors controlling nitrate dynamics and potential denitrification hot spots and hot moments in groundwater of an alluvial floodplain. Ecol. Eng. 103, 372–384.
Blake, G.R., Hartge, K.H., 1986. Bulk Density. In: Klute, A. (Ed.), Methods of Soil Analysis, Part 1: Physical and Mineralogical Methods. Soil Science Society of America, Madison, WI, pp. 363–376.
Bledsoe, C.S., Fahey, T.J., Day, F.P., Ruess, R.W., 1999. Measurement of Static Root Parameters: Biomass, Length, and Distribution in the Soil Profile. In: Robertson, G.P., Coleman, D.C., Bledsoe, C.S., Sollins, P. (Eds.), Standard Soil Methods for Long-Term Ecological Research. Oxford University Press, New York, NY, pp. 413–436.
Burgin, A.J., Groffman, P.M., Lewis, D.N., 2010. Factors regulating denitrification in a riparian wetland. Soil Sci. Soc. Am. J. 74, 1826–1833.
Cabezas, A., Comín, F.A., 2010. Carbon and nitrogen accretion in the topsoil of the Middle Ebro River floodplains (NE Spain): implications for their ecological restoration. Ecol. Eng. 36, 640–652.
Carbonneau, P., Fonstad, M.A., Marcus, W.A., Dugdale, S.J., 2012. Making riverscapes real. Geomorphology 137, 74–86.
Chabot, H., Farrow, D., York, D., Harris, J., Cosentino-Manning, N., Watson, L., Hum, K., Wiggins, C., 2016. Thinking big: lessons learned from a landscape-scale approach to coastal habitat conservation. Coast. Manag. 44 (3), 175–192.
Chesapeake Bay Program, 2012. CBP Water Quality Database (1984–Present). http://www.chesapeakebay.net/data/downloads/cbp_water_quality_database_1984_present.
Chesapeake Conservancy, 2017. Chesapeake Bay land Cover Data. http://chesapeakeconservancy.org/.
Craft, C., Megononigal, P., Broome, S., Stevenson, J., Freese, R., Cornell, J., Zheng, L., Sacco, J., 2003. The pace of ecosystem development of *Spartina alterniflora* marshes. Ecol. Appl. 13 (5), 1417–1432.
Cummins, J., et al., 2010. Potomac basin large river environmental flow needs. In: The Nature Conservancy of Maryland. ICPRB report 10-3.
Denver, J.M., et al., 2004. Water Quality in the Delmarva Peninsula, Delaware, Maryland, and Virginia, 1999–2001. U.S. Geological Survey, Circular 1228.
Duncan, J.M., Groffman, P.M., Band, L.E., 2013. Towards closing the watershed nitrogen budget: spatial and temporal scaling of denitrification. J. Geophys. Res. Biogeosci. 118, 1105–1119.
Falciani, R., Novaro, E., Marchesini, M., Gucciardi, M., 2000. Multi-element analysis of soil and sediment by ICP-MS after a microwave assisted digestion method. J. Anal. At. Spectrom. 5, 561–565.
Forshay, K.J., Stanley, E.H., 2005. Rapid nitrate loss and denitrification in a temperate river floodplain. Biogeochemistry 75, 43–64.
Fowler, D., et al., 2013. The global nitrogen cycle in the twenty-first century. Philos. T. R. Soc. B. 368, 20130164. https://doi.org/10.1098/rstb.2013.0164.
Gardner, W.H., 1996. Water content. In: Sparks, D.L. (Ed.), Methods of Soil analysis. Part 3: Chemical Methods. Soil Science Society of America, Madison, WI, pp. 961–1010.
Gellis, A.C., et al., 2009. Sources, Transport, and Sources of Sediment at Selected Sites in the Chesapeake Bay Watershed. U.S. Geological Survey. Scientific Investigations 2008-5186. (95 p).
Gordon, N.D., McMahon, T.A., Finlayson, B.L., Gippel, C.J., Nathan, R.J., 2004. Stream Hydrology: And Introduction for Ecologists, Second edition. John Wiley & Sons, Chichester, England.
Groffman, P.M., Crawford, M.K., 2003. Denitrification in urban riparian zones. J. Environ. Qual. 32, 1144–1149.
Groffman, P.M., Tiedje, J.M., Mokma, D.L., Simkins, S., 1992. Regional scale analysis of denitrification in north temperate forest soils. Landsc. Ecol. 7 (1), 45–53.
Groffman, P.M., Holland, E.A., Myrold, D.D., Robertson, G.P., Zou, X., 1999. Denitrification. In: Robertson, G.P., Coleman, D.C. (Eds.), Standard Soil Methods for Long-Term Ecological Research. Oxford University Press, Inc., New York.
Groffman, P.M., Tiedje, J.M., Mokma, D.L., Simkins, S., 2002. Soil nitrogen cycle processes in urban riparian zones. Environ. Sci. Technol. 36 (21), 4547–4552.
Harms, T.K., Grimm, N.B., 2008. Hot spots and hot moments of carbon and nitrogen dynamics in a semiarid riparian zone. J. Geophys. Res. G01020. https://doi.org/10.1029/2007JG000588.
Harrison, M.D., Groffman, P.M., Mayer, P.M., Kaushal, S.S., Newcomer, T.A., 2011. Denitrification in alluvial wetlands in an urban landscape. J. Environ. Qual. 40, 634–646.
Harvey, J., Gooseff, M., 2015. River corridor science: hydrologic exchange and ecological consequences from bedforms to basins. Water Resour. Res. 51, 6893–6922.
Heffernan, J.B., et al., 2014. Macrosystems ecology: understanding ecological patterns and processes at continental scales. Front. Ecol. Environ. 12 (1), 5–14.
Hefting, M., et al., 2004. Water table elevation controls on soil nitrogen cycling in riparian wetlands along a European climatic gradient. Biogeochemistry 67, 113–134.
Hill, A.R., Devito, K.J., Campagnolo, S., Sanmugadas, K., 2000. Subsurface denitrification in a forest riparian zone: interactions between hydrology and supplies of nitrate and organic carbon. Biogeochemistry 51, 193–223.
Hoffman, C.C., Kjaergaard, C., Uusi-Kämppä, J., Hansen, H.C.B., Kronvang, B., 2009. Phosphorus retention in riparian buffers: review of their efficiency. J. Environ. Qual. 38, 1942–1955.
Hogan, D.M., Walbridge, M.R., 2007. Urbanization and nutrient retention in freshwater riparian wetlands. Ecol. Appl. 17 (4), 1142–1155.
Hopkins, K.G., et al., 2015. Assessment of regional variation in streamflow responses to urbanization and the persistence of physiography. Environ. Sci. Technol. 49 (5), 2724–2732.
Hopkins, K.G., et al., 2018. A method to quantify and value floodplain sediment and nutrient retention ecosystem services. J. Environ. Manag. 220, 65–76.
Hupp, C.R., Noe, G.B., Schenck, E.R., Benthem, A.J., 2013. Recent and historic sediment dynamics along difficult run a suburban Virginia Piedmont stream. Geomorphology 180–181, 156–169.
Hupp, C.R., Dufour, S., Bornette, G., 2016. Vegetation as a tool in the interpretation of fluvial geomorphic processes and landforms. In: Shroder, J.F. (Ed.), Treatise on Geomorphology. Volume 12. Ecogeomorphology. Academic Press, San Diego, CA.
Kaase, C.T., Kupfer, J.A., 2016. Sedimentation patterns across a coastal plain floodplain: the importance of hydrogeomorphic influences and cross-floodplain connectivity. Geomorphology 269, 43–55.
Keddy, K.R., DeLaune, R.D., 2008. Biogeochemistry of Wetlands: Science and Applications. CRC Press, Boca Raton, FL.
Knowles, R., 1990. Acetylene inhibition technique: development advantages, and potential problems. In: Revsbech, N.P., Sórensen, J. (Eds.), Denitrification in Soil and Sediment. Plenum Press, New York, NY, pp. 151–166.
Korol, A.R., Ahn, C., Noe, G.B., 2016. Richness, biomass, and nutrient content of a wetland macrophyte community affect soil nitrogen cycling in a diversity-ecosystem functioning experiment. Ecol. Eng. 95, 252–265.
Kulkarni, M.V., Groffman, P.M., Yavitt, J.B., Goodale, C.L., 2014. Complex controls of denitrification at ecosystem, landscape, and regional scales in northern hardwood forests. Ecol. Model. 298 (24), 39–52.
Langland, M.J., Cronin, T., 2003. A summary report of sediment processes in Chesapeake Bay and watershed, U.S. Geological Survey Water-Resources Investigations Report. 2003 (4123). https://pubs.er.usgs.gov/publication/wri034123.
Langland, M.J., Blomquist, J.D., Moyer, D.K., Hyer, K.E., Chanat, J.G., 2013. Total nutrient and sediment loads, trends, yields and nontidal water-quality indicators for selected nontidal stations, Chesapeake Bay watershed, 1985–2011. In: U.S. Geological Survey. Report 2013-1052.
Legendre, P., Legendre, L., 2012. Numerical Ecology, 3rd edition. Elsevier, Amsterdam, The Netherlands.
Lowrance, R., et al., 1997. Water quality functions of riparian forest buffers in Chesapeake Bay watersheds. Environ. Manag. 21 (5), 687–712.
Machefert, S.E., Dise, N.B., 2004. Hydrological controls on denitrification in riparian ecosystems. Hydrol. Earth Syst. Sci. 8 (4), 686–694.
McClain, M.E., et al., 2003. Biogeochemical hot spots and hot moments at the interface of terrestrial and aquatic ecosystems. Ecosystems 6, 301–312.
McCluney, K.E., et al., 2014. Riverine macrosystems ecology: sensitivity, resistance, and resilience of whole river basins with human alterations. Front. Ecol. Environ. 21 (1), 48–58.
McMillan, S., Noe, G., 2017. Increasing floodplain connectivity through urban stream restoration to improve nutrient and sediment retention. Ecol. Eng. 108, 284–294.
McPhillips, L.E., Groffman, P.M., Goodale, C.L., Walter, M.T., 2015. Hydrologic and biogeochemical drivers of riparian denitrification in an agricultural watershed. Water. Air. Soil. Poll. 226, 169.
Megonigal, J.P., Neubauer, S.C., 2009. Biogeochemistry of tidal freshwater wetlands. In: Perillo, G. (Ed.), Coastal Wetlands: An Integrated Ecosystem Approach. Amsterdam, The Netherlands.
Merrill, A.G., Benning, T.L., 2006. Ecosystem type differences in nitrogen process rates and controls in the riparian zone of a montane landscape. For. Ecol. Manag. 222, 145–161.
Messer, T.L., Burchell, M.R., Grabow, G.L., Osmond, D.L., 2012. Groundwater nitrate reductions within upstream and downstream sections of a riparian buffer. Ecol. Eng. 47, 297–307.
Mitsch, W.J., Gosselink, J.G., 2015. Wetlands, fifth edition. John Wiley & Sons, Inc., Hoboken, NJ.
Muthén, Muthén, 2013. Mplus Version 7.11 [Computer Software]. Los Angeles, California.
Nelson, D.W., Sommers, L.E., 1996. Total carbon, organic carbon, and organic matter. In: Sparks, D.L. (Ed.), Methods of Soil Analysis. Part 3: Chemical Methods. Soil Science Society of America, Madison, WI, pp. 961–1010.
Noe, G.B., 2013. Interactions among hydrogeomorphology, vegetation, and nutrient biogeochemistry in floodplain ecosystems. In: Shroder, J.F. (Ed.), Treatise on Geomorphology. Volume 12. Academic Press, San Diego, CA, Ecogeomorphology, pp. 307–321.
Noe, G.B., Hupp, C.R., 2005. Carbon, nitrogen, and phosphorus accumulation in floodplains of Atlantic Coastal Plain rivers, USA. Ecol. Appl. 15 (4), 1178–1190.
Noe, G.B., Hupp, C.R., 2007. Seasonal variation in nutrient retention during inundation of a short-hydroperiod floodplain. River Res. Appl. 23, 1088–1110.
Noe, G.B., Hupp, C.R., Rybicki, N.B., 2013. Hydrogeomorphology influences soil nitrogen and phosphorus mineralization in floodplain wetlands. Ecosystems 16, 75–94.
Opperman, J.J., Luster, R., McKenney, B.A., Roberts, M., Meadows, A.W., 2010. Ecologically functional floodplains: connectivity, flow regime, and scale. J. Am. Water Resour. Assoc. 46 (2), 211–226.
Pahlavan-Rad, M.R., Akbarimoghaddam, A., 2018. Spatial variability of soil texture fractions and pH in a floodplain (case study from eastern Iran). Catena 160, 275–281.
Parrett, C., Johnson, D.R., 2004. Methods for estimating flood frequency in Montana based on data through water year 1998. In: U.S. Geological Survey. Water-Resources Investigations Report 03-4308.
Pinay, G., Black, V.J., Planty-Tabacchi, A.M., Gumiero, B., Décamps, H., 2000. Geomorphic control of denitrification in large river floodplain soils. Biogeochemistry 50 (2), 163–182.
Pinay, G., et al., 2007. Patterns of denitrification rates in European alluvial soils under

various hydrological regimes. Freshw. Biol. 52, 252–266.
PRISM Climate Group, 2017. Oregon State University. http://www.prism.oregonstate.edu.
R Core Team, 2015. R: A Language and Environment for Statistical Computing. R Foundation for Statistical Computing, Vienna, Austria. https://www.r-project.org/.
Reddy, K.R., DeLaune, R.D., 2008. Biogeochemistry of Wetlands: Science and Applications. Taylor & Francis Group, Boca Raton, Florida.
Rivett, M.O., Buss, S.R., Morgan, P., Smith, J.W.N., Bemment, C.D., 2008. Nitrate attenuation in groundwater: a review of biogeochemical controlling processes. Water Res. 42, 4215–4232.
Robertson, G.P., Groffman, P.M., 2015. Nitrogen transformations. In: Paul, E.A. (Ed.), Soil Microbiology, Ecology and Biochemistry, Fourth edition. Academic Press, Burlington, MA.
Robertson, G.P., Sollins, P., Ellis, B.G., Lajtha, K., 1999a. Exchangeable ions, pH, and cation exchange capacity. In: Robertson, G.P., Coleman, D.C., Bledsoe, C.S. (Eds.), Standard Soil Methods for Long-Term Ecological Research. Oxford University Press, New York, New York, pp. 106–114.
Robertson, G.P., Wedin, D., Groffman, P.M., Blair, J.M., Holland, E.A., Nadelhoffer, K.J., Harris, D., 1999b. Soil carbon and nitrogen availability: nitrogen mineralization, nitrification, and soil respiration potentials. In: Robertson, G.P., Coleman, D.C., Bledsoe, C.S. (Eds.), Standard Soil Methods for Long-Term Ecological Research. Oxford University Press, New York, New York, pp. 258–271.
Rosgen, D.L., 1994. A classification of natural rivers. Catena 22, 169–199.
Saint-Laurent, D., et al., 2016. Impacts of floods on organic carbon concentrations in alluvial soils along hydrological gradients using a digital elevation model (DEM). Water. 8, 208.
Saleh-Lakaha, S., Pardis, R., Drouin, A., Gervais-Beaulac, V., 2009. Effect of pH and temperature on denitrification gene expression and activity in *Pseudomonas mandelii*. Appl. Environ. Microbiol. 75 (12), 3903–3911.
Schenk, E.R., et al., 2013. Geomorphic change on the Missouri River during the flood of 2011. In: U.S. Geological Survey Professional Paper, 1798-I, . https://pubs.usgs.gov/pp/1798/.
Schilling, E.B., Lockaby, B.G., 2005. Microsite influences on productivity and nutrient circulation within two southeastern floodplain forests. Soil Sci. Soc. Am. J. 69, 1185–1195.
Schwartz, S.S., Smith, B., McGuire, M.P., 2012. Baseflows Signatures of Sustainable Water Resources: An Analysis of Maryland Streamflow. Hughes Center for Agro-Ecology Research, Queenstown, MD.
Sherwood, W.C., Garst, F.M., 2016. Soils of Virginia. In: Bailey, C.M., Sherwood, W.C., Eaton, L.S., Powers, D.S. (Eds.), The Geology of Virginia. Virginia Museum of Natural History, Martinsville, VA, pp. 291–313.
Shrestha, J., et al., 2014. Flood pulses control soil nitrogen cycling in a dynamic river floodplain. Geoderma 228–229, 14–24.
Steiger, J., Gurnell, A.M., 2002. Spatial hydrogeomorphological influences on sediment and nutrient deposition in riparian zones: observations from the Garonne River, France. Geomorphology 49, 1–23.
Sutton-Grier, A., Wright, J.P., Richardson, C.J., 2013. Different plant traits affect two pathways of riparian nitrogen removal in a restored freshwater wetland. Plant Soil 365, 41–57.
Thoms, M.C., Parsons, M., 2002. Eco-geomorphology: an interdisciplinary approach to river science. In: Cudennec, C. (Ed.), The Structure, Function, and Management Implications of Fluvial Sedimentary Systems. Copernicus Publications, Göttingen, Germany, pp. 113–119.
Thorp, J.H., Thoms, M.C., Delong, M.D., 2006. The riverine ecosystem synthesis: biocomplexity in river networks across space and time. River Res. Appl. 22, 123–147.
Tiner, R.W., 1999. Wetland Indicators: A Guide to Wetland Identification, Delineation, Classification, and Mapping. CRC Press, Boca Raton, FL.
Tomasek, A., 2017. Environmental drivers of denitrification rates and denitrifying gene abundances in channels and riparian areas. Water Resour. Res. 53, 6523–6538.
U.S. Environmental Protection Agency, 2010. Guidance for Federal Land Management in the Chesapeake Bay watershed. EPA841-R-10-002. https://www.epa.gov/nps.
U.S. Geological Survey, 2016. National water information system data. http://waterdata.usgs.gov/nwis/.
van Groenigen, J.W., Huygens, D., Boeckx, P., Kuyper, Th.W., Lubbers, I.M., Rütting, T., Groffman, P.M., 2015. The soil N cycle: new insights and key challenges. Soil 1, 235–256.
Vidon, P., et al., 2010. Hot spots and hot moments in riparian zones: potential for improved water quality management. J. Am. Water Resour. Assoc. 46 (2), 278–298.
Vogt, E., et al., 2015. Catchment land use effects on fluxes and concentrations of organic and inorganic nitrogen in streams. Agric. Ecosyst. Environ. 199, 320–332.
Walsh, C.J., Roy, A.H., Feminella, J.W., Cottingham, P.D., Groffman, P.M., Morgan, R.P., 2005. The urban stream syndrome: current knowledge and the search for a cure. J. N. Am. Benthol. Soc. 24 (3), 706–723.
Wassen, M.J., OldeVenterink, H., 2006. Comparison of nitrogen and phosphorus fluxes in some European fens and floodplains. Appl. Veg. Sci. 9, 213–222.
Wassen, M.J., et al., 2002. Patterns in vegetation, hydrology, and nutrient availability in an undisturbed river floodplain in Poland. Plant Ecol. 165, 27–43.
Waters, E.R., Peeters, W.H.M., Olde Venterink, H., 2014. Differential carbon and nitrogen controls of denitrification in riparian zones and streams along a urban to exurban gradient. J. Environ. Qual. 43, 955–963.
Welsh, M.K., et al., 2017. Denitrification along the stream-riparian continuum in restored and unrestored agricultural streams. J. Environ. Qual. 46, 1010–1019.
Wilson, J.S., McMillan, S.K., Vidon, P.G., 2011. The effects of short-term inundation on carbon dynamics, microbial community structure and microbial activity in floodplain soil. River Res. Appl. 27, 213–225.
Winter, T.C., 2001. The concept of hydrologic landscapes. J. Am. Water Resour. Assoc. 37 (2), 335–349.
Wolf, K.L., Noe, G.B., Ahn, C., 2013. Hydrologic connectivity to streams increases nitrogen and phosphorus inputs and cycling in soils of created and natural floodplain wetlands. J. Environ. Qual. 42, 1245–1255.
Zedler, J.B., 2003. Wetlands at your service: reducing impacts of agriculture at the watershed scale. Front. Ecol. Environ. 1 (2), 65–72.
Zuur, A.F., Leno, E.N., Walker, N., Saveliev, A.A., Smith, G.M., 2009. Mixed Effects Models and Extensions in Ecology in R. Springer, New York, NY.